DTIC
S **ELECTE**
JAN 1 2 1994
C **D**

AD-A274 643

JOINT SERVICES ELECTRONICS PROGRAM

Sixteenth Annual Report

The Ohio State University

ElectroScience Laboratory

Department of Electrical Engineering
Columbus, Ohio   43212

94 1 10 170

94-01202

NOTICES

When Government drawings, specifications, or other data are
used for any purpose other than in connection with a definitely
related Government procurement operation, the United States
Government thereby incurs no responsibility nor any obligation
whatsoever, and the fact that the Government may have formulated,
furnished, or in any way supplied the said drawings, specifications,
or other data, is not to be regarded by implication or otherwise as
in any manner licensing the holder or any other person or corporation,
or conveying any rights or permission to manufacture, use, or sell
any patented invention that may in any way be related thereto.

80272-101

REPORT DOCUMENTATION PAGE	1. REPORT NO.	2.	3. Recipient's Accession No.
4. Title and Subtitle Joint Services Electronics Program - Sixteenth Annual Report			5. Report Date November 1993
			6.
7. Author(s) Leon Peters, Jr.			8. Performing Org. Rept. No. 721563-6
9. Performing Organization Name and Address The Ohio State University ElectroScience Laboratory 1320 Kinnear Road Columbus, OH 43212			10. Project/Task/Work Unit No.
			11. Contract(C) or Grant(G) No. (C) N00014-K-1007 (G)
12. Sponsoring Organization Name and Address Department of the Navy, Office of Naval Research 800 North Quincy Street Arlington, Virginia 22217			13. Report Type/Period Covered Annual Report
			14.

15. Supplementary Notes

16. Abstract (Limit: 200 words)

17. Document Analysis   a. Descriptors

b. Identifiers/Open-Ended Terms

c. COSATI Field/Group

18. Availability Statement A. Approved for public release; Distribution is unlimited.	19. Security Class (This Report) Unclassified	21. No. of Pages 71
	20. Security Class (This Page) Unclassified	22. Price

(See ANSI-Z39.18)   *See Instructions on Reverse*   OPTIONAL FORM 272 (4-77)
Department of Commerce

Contents

List of Figures

I. DIRECTOR'S OVERVIEW

This report represents the sixteenth annual summary of The Ohio State University Joint Services Electronics Program (JSEP).

There have been a total of 33 Ph.D. and 24 M.Sc. degrees in Electrical Engineering obtained under partial JSEP sponsorship. There are currently 6 Ph.D. and 3 M.Sc. students being partially supported under JSEP.

As may be seen in the Annual Report Appendix, 10 reprints have been included for the period September 1992 to September 1993. In addition, 6 papers have already been accepted for publication in the coming year, an additional 11 papers have been submitted, and an additional 16 papers are in preparation.

II. DESCRIPTION OF SPECIAL ACCOMPLISH-MENTS AND TECHNOLOGY TRANSITION

The transfer of the compact range and target identification technology initiated under JSEP support for time domain studies continues to make large advances. The installation of a large compact reflector and a modern radar of our design has been completed for ASD at Wright Patterson Air Force Base. This system will have all of the sensitivity of the Mini Range reported last year and yet has a 14' quiet (or target) zone. The reflector includes all the most updated features of the ESL design. Dr. Brian Kent of ASD has expressed complete satisfaction with its performance. It is the range we would like to have, but can never afford. A large even more advanced compact range is currently being designed for NASA, Langley which is specifically being focussed for measurements as low as 300 MHz. This new range will fit in a room 40' × 40' × 80' instead of the previously required 120' × 120' × 360'. The cost savings in this case are enormous.

We continue to assist Rockwell (Tulsa) to update their RCS facilities. This work is on a subcontract to the ESL from the Air Force. These and other advances were only possible because of the initial JSEP support. This continues to be a case where a small investment of basic research funds have been leveraged to generate much larger support and have achieved

major contributions for DoD. This has also lead to OSU-ESL involvement in the study of Ultra Wide Band radar systems.

Our target identification work, also partially funded at one time under JSEP Time Domain Studies, is also being funded by several other agencies including Naval EOD Technology Center and continues to be rather vigorous. Our focus here is on the detection of unexploded ordnance which is a natural for the Complex Natural Resonance Techniques developed under JSEP. While these studies are directed at Ground Penetrating Radar Design, some minor effort is focussed on the target identification. We seek more robust techniques than have previously been developed. Several new concepts already under consideration indicate that a more directed research program in this area merits consideration. Again, JSEP funds have been leveraged to initiate larger programs which have been supported continuously since JSEP funding was terminated.

The research activities devoted to the Generalized Ray and Gaussian Beams continues to be expanded by external funding. This program is being expanded by use of such funds which are more focussed on the requirements of the sponsors which include both the Air Force and the Navy.

It becomes clear from the above that a major portion of technology transition of JSEP research takes the form of additional supported research from other DoD agencies. Other forms of transition include former graduate students, who upon graduation are employed in DoD related positions, and publications of results of JSEP research. Yet another form of such transition is represented by computer codes that incorporate the results of our research. These complex codes are available to DoD related industries for a nominal fee of $250. Last year 65 such codes were issued.

Our JSEP research continues to focus on electromagnetic related topics. There are four major electromagnetics areas that were pursued in the past year.

The Diffraction Studies Work Unit has continued research on a time domain version of the Uniform Theory of Diffraction. This time domain version (TD-UTD) has a major potential flaw when the rays pass through a caustic, in that the fields become non-causal. However, the fields in the causal region are correctly predicted. This has led to the development of a means of discarding the non-causal component which appears to be successful. More

2

examples are being considered to further establish the validity of this development. This TD-UTD solution should be most useful in predicting the early to intermediate time signals and providing physical insight to various scattering processes.

The introduction of the Equivalent Current Method (ECM) and/or the Incremental Theory of Diffraction (ITD) which is useful in patching up the UTD in regions of diffracted ray caustics has led to a time domain version for diffraction which is causal and which thus provides in those situations an alternative to the procedure mentioned earlier for obtaining causal responses. These techniques are designated as TD-ECM or TD-ITD and are being tested initially on simple configurations; their development will next be focussed on more general and thus also more complex radiating/scattering bodies.

Research in the Diffraction Studies Work Unit has continued on extensions of the Generalized Resistive Boundary Condition (GRBC) and the Generalized Impedance Boundary Condition (GIBC). A generalized edge/junction condition is introduced to ensure uniqueness and satisfy reciprocity. A synthesis algorithm has been developed to obtain a desired resistive termination to control diffraction from an edge.

A third topic in the Diffraction Studies Work Unit involves the development of new asymptotic canonical solutions. One of these is for a magnetic point current source on an elongated smooth perfectly conducting convex surface when the observer is located in the paraxial region. This makes it practical to extend the usefulness of diffraction concepts to the paraxial (or near end fire) region where UTD has failed. This is an extremely significant step and its usefulness is now being scrutinized. Another canonical solution is the diffraction of an inhomogeneous (non-uniform and complex) plane wave by an impedance wedge. This solution indicates that the shadow boundaries (which are a controlling factor in diffraction theory) are quite different from those of a similar wedge which is excited by a conventional real (or homogeneous) plane wave.

A fourth task involves the reflection/diffraction of a Gaussian beam. Last year, it was noted that this represents an approach to replace the usual ray optics solution for very complex geometries where the versatile ray optics solution becomes cumbersome. The two dimensional (2-D) Gaussian Beam Diffraction (GB) by an edge has now been extended so that it remains valid in the near zone just as the 2-D and 3-D GB reflection does. In the

3

3-D reflection case, the GB can exhibit general astigmatic effects. Diffraction of rotationally symmetric GB's by an edge in a 3-D curved screen has also been analyzed when the plane of incidence is coincident with principal directions on the curved surface. Next, this solution is to be extended to deal with the diffraction by general 3-D astigmatic GB's. It is noted that conventional complex source point (CSP) techniques, which are sometimes used for generating GB's in 2-D, and also rotationally symmetric 3-D GB's, cannot be directly applied to represent general 3-D astigmatic GB's and hence it becomes necessary to develop useful techniques different from the CSP based methods to deal with the reflection and diffraction of astigmatic GB's as are being pursued in this research.

Finite element techniques represent an area where the electromagnetics community has focussed much attention in the past few years. They are particularly suited for analyzing the scattering from penetrable bodies of arbitrary shape with arbitrary inhomogeneities. However, the ultimate goal of treating 3-D targets that are very large in terms of wavelength has not been achieved. Research under this work unit was focussed on three approaches for extending the capability of the finite element techniques.

First, the work on the bymoment method has now been completed and some typical results are compared with alternate solutions for a sphere, a lossy dielectric prolate spheroid, and a dielectric cube. The bymoment method is a rigorous boundary truncation technique which does not suffer the disadvantage of the approximate absorbing boundary conditions. Namely, in the bymoment method, the grid can be placed close to the scatterer. The bymoment method is also more efficient than a traditional coupled finite element/boundary integral formulation. The efficiency is due to the fact that the boundary solution in the bymoment method is decoupled from the finite element solution, whereas the boundary solution in the finite element/boundary integral is directly coupled to the finite element solution, reducing the sparsity of the finite element matrix.

Second, the measured equation of invariance (MEI), which was developed by Ken Mei at Berkeley has been analyzed. The MEI is a boundary truncation technique which Mei claims is rigorous for modeling perfectly conducting bodies while being much more efficient than current rigorous techniques including the bymoment method. In the analysis, we show that MEI is still only an approximate boundary condition and that its accuracy is based on the

4

choice of certain parameters. The analysis given in this report provides a systematic way of choosing these parameters for producing good results. For 2-D convex geometries, MEI has been very successful at producing accurate solutions. A numerical study has been done to explain the reasons for this accuracy, and this study is presented in the accompanying paper. The MEI has also been extended to model scattering from bodies of revolution. The results are not as good as in the 2-D case. However, they are still reasonable. Results are shown for a finite conducting cylinder and a conducting cone.

In the third part of this effort, the partitioning technique which was developed in the previous year is modified to more efficiently model electrically large structures. The partitioning techniques segments the structure into many sections. The finite element solution within each sections is generated independent of the other sections. The sections are then coupled to produce the correct solution. The biggest advantage of this approach is that the computer memory is reduced by an order of magnitude or more for large targets. Also, the method is ideally suited for parallelization.

The Integral Equations Work Unit has been focussed on evaluating the electrical properties of a 3-D artificial dielectric where the artificial media has been constructed from a variety of periodic shapes (rods, loops, crosses, tees, etc.). Last year, the analysis was reported for a 3-D periodic array of small spheres. Both the permittivity and the loss tangent were evaluated. This year, we completed the analysis for an anisotropic array of wires. This now leads to solutions for the electrical properties of composites. The results for a dielectric wave pattern are given as an example. This is to be applied to typical composite structures in the future. These results should be of great value to anyone using composites for analyzing their electrical properties.

The Hybrid Studies Work Unit involves a cooperative effort for most of the researchers involved in other work units. The goal is to combine techniques for radiation/scattering from geometries for which no single solution would be practically possible. In the past UTD-MM and MM-UTD solutions have been developed and are currently being employed to analyze stripline antennas. Analytical methods with the generalized scattering matrix are also under development as are hybrid combinations of high frequency ray techniques with the Finite Difference Time Domain (FDTD) solutions. The combinations of these various methods

5

each offer unique possibilities to further understanding and evaluation of scattering/radiation mechanisms. Current research has involved a number of important tasks. The main goal of this includes analyzing electromagnetic phenomena associated with large complex structures and the influence of materials on these phenomena. Topics covered in this past year: 1) Analysis of conformal antennas, 2) radiation/coupling associated with antennas in a complex environment, 3) radiation/scattering from airborne/spaceborne objects, 4) scattering from an impedance wedge in the presence of a material body, 5) planar guided wave structures, and 6) ray-FDTD method for inlet cavities.

The conformal antennas study involves the analysis of large but finite arrays of strip line antennas mounted on grounded substrates. Any brute force analysis (integral equations, finite difference or any other isolated solution) becomes intractable for large arrays. The hybrid solution (an MM-UTD form) is based on a UTD-like closed asymptotic form of the grounded slab Green's function. This should make it practical to replace the commonly used infinite periodic array treatment and thus be better able to analyze finite arrays and arrays mounted on surfaces with variable radii of curvature.

Radiation of large antennas in a complex environment has been of interest to the Navy for ships for many years. Combining the generalized ray expansion and the Gaussian beam technology appears to be leading to a tractable solution to this complex task where the antenna beam must be scanned through a bewildering structure of masts and antennas, etc.

Evaluating radiation/scattering from airborne/spaceborne objects is indeed a complex task that has faced the Air Force for many years and has become even more involved when modern complex materials are included. There is a Tri-Service Electromagnetic Code Consortium (EMCC) that is currently attacking this task via "brute" force techniques, using finite difference/element solutions on ever larger, faster parallel computers. It is apparent that these solutions will face limits on size, frequency and accuracy. The MM-UTD hybrid solutions under study should make it practical to generate accurate estimates in the regime where the previous solutions will fail.

The hybrid analysis of an impedance wedge in the presence of a material body will make it possible to treat more realistic representations of practical structures. The crucial element of this study is to obtain a numerically efficient asymptotic form of the appropriate Green's

function so that the associated moment method solution will contend with a minimum number of unknowns. Of course, practical structures may be material-coated wings, stabilizers, etc.

The hybrid analysis of planar, guided wave structures has been conducted via a combination of Wiener Hopf and Generalized Scattering Matrix Techniques (WH/GSMT) and is applicable to transmission lines with large lateral dimensions. It will complement existing schemes which are more efficient for small structures. An application of this study, besides being able to predict the modal structure for these guides, is to be able to combine it with the analysis of planar patch or slot antenna arrays where such guided wave structures can serve as feed lines (for the radiating array elements). An efficient hybrid solution of an integral equation formulation of the combined antenna array and feed structure can be obtained if one employs the few propagating and evanescent modes as the basis functions to represent the unknown current on the feed lines as opposed to using a large number of conventional subsectional basis functions over the entire feed structure. It is noted that most previous analyses of planar guided wave structures are restricted to the dominant mode case. In contrast, the present WH/GSMT hybrid scheme can be employed to obtain the higher order modes of such structures. The integration of antenna arrays and feed lines is planned during the future phases of this study.

Finally, the ray/FDTD method for treating inlet cavities is focussed on a very difficult task where the engine interface terminates an inlet cavity. Previous solutions relied on some highly approximate techniques, or on rigorous techniques applicable to relatively simple body of revolution type terminations to obtain the reflection from the interface. In this current hybrid solution, GRE is used to model the ducts and the FDTD is used to model the very complex engine termination. This is extremely important since the jet inlets/engines represent dominant scatterers in modern aircraft.

III. DIFFRACTION STUDIES

Researchers:

R.G. Kouyoumjian, Professor   (Phone: 614/292-7302)
P.H. Pathak, Professor   (Phone: 614/292-6097)
R. Rojas, Senior Research Associate   (Phone: 614/292-2530)
R.J. Burkholder, Post-Doctoral Researcher (Phone: 614/294-4597)
G. Zogbi, Graduate Research Associate (Phone: 614/294-9283)

1. Introduction

One of the research topics currently under investigation in diffraction studies deals with the development of a time-domain version of the uniform geometrical theory of diffraction (TD-UTD). Such a TD-UTD should provide a simple progressive wave picture for describing the phenomenon of transient electromagnetic (EM) radiation and scattering. A TD-UTD would thereby yield essentially the same physical insight into these wave phenomena as that given by the simple ray picture of the uniform geometrical theory of diffraction (UTD) which has been developed originally in the frequency domain (or continuous wave case). The UTD was developed primarily at The Ohio State University [1]–[4] largely under past JSEP support. This UTD development was essential for making the ray methods work successfully in analyzing practical EM antenna and scattering configurations. The systematic introduction of special functions (characteristic of the diffraction processes which can occur in such configurations) in the UTD development allows it to patch up the conventional geometrical theory of diffraction (GTD), which was developed previously by Keller [5], within the ray shadow boundary transition regions where the GTD fails. Initially, Keller developed GTD expressions for describing the diffraction by edges and smooth convex boundaries which were perfectly conducting. The UTD [1]–[4] procedure then subsequently extended the GTD for diffraction by perfectly conducting edges and convex surfaces for use even in shadow boundary transition regions as well as to deal with the radiation and mutual coupling between antennas on smooth convex perfectly conducting surfaces, and even more recently to deal with the diffraction of waves by perfectly conducting corners, and even by edges in non-

8

conducting surfaces. These extensions have made the UTD applicable to the analysis of many complex radiating (antenna/scattering) configurations which can be built up from straight or curved edges, convex boundaries, vertices, etc. It is important to note that the frequency domain UTD solutions are important to the development of the TD-UTD since the TD-UTD is being developed via an analytical inversion of the frequency domain UTD solutions into the time domain (using a Fourier or Laplace inversion). Thus, additional developments in the UTD are essential not only to accurately predict the EM performance of a wider class of complex radiating systems than is currently possible, but also to accurately predict the early to intermediate time transient response of those same complex radiating systems when they are now excited by pulsed sources. An analytical TD-UTD solution would be far more efficient and physically transparent than a numerical Fast Fourier Transform (FFT) inversion of the frequency domain solutions to obtain the corresponding time domain solutions.

Direct time domain solutions are of great importance and interest in the area of short pulse technology for radar target identification, remote sensing and other applications. At present, a TD-UTD solution has been obtained for predicting the transient diffraction by an edge in an otherwise smooth convex perfectly conducting surface; this has been achieved by extending the TD-UTD solution for the special case of a straight, perfectly conducting edge given earlier by Verrutipong and Kouyoumjian [6]. However, this TD-UTD solution for a curved wedge can lead to a non-causal result for the transient diffracted field produced by an impulsive plane wave illumination of the wedge if the diffracted ray in the corresponding frequency domain UTD solution (used in the development of the TD-UTD result) traverses a diffracted ray caustic before arriving at the observation point. Such non-causal results can also occur in the transient reflection contribution from a smooth surface if the geometrical optics (GO) reflected ray in the corresponding UTD solution (which contains GO as its leading term) passes through a smooth caustic of reflected rays before arriving at the observation point. These non-causal effects are presently under study and some steps to overcome this limitation of the analytical TD-UTD solutions have been achieved, but they need to be tested further with appropriate reference solutions as discussed later in the slightly more detailed description of the present accomplishments in the area of diffraction studies. The latter description will also include some recent analytical developments which

9

have led to a new frequency domain UTD solution for the radiation within the paraxial region of a smooth, elongated perfectly-conducting convex body containing a conformal slot antenna. This important result is not only useful in its own right for the analysis of conformal antennas and antenna arrays on smooth elongated bodies, but it can also provide the basis for the construction of another related and important UTD solution for the paraxial diffraction by smooth, elongated perfectly conducting bodies excited by nearby antennas. In addition, it can be used to significantly simplify the development of a hybrid solution for the radiation and scattering by modern aircraft and missile structures (see description of work reported under Hybrid Studies). Another important canonical frequency-domain UTD solution which has been developed recently is for the diffraction of an inhomogeneous pla .e wave by an impedance wedge. It is expected that this UTD solution for inhomogeneous (or complex) plane wave diffraction will become useful in dealing with the modeling of underground wave propagation in lossy regions containing highly conducting wedge-like inhomogeneities. Such a UTD solution is also expected to be useful in the development of efficient solutions to describe the diffraction by edges and other related configurations when they are illuminated by Gaussian beams, since the latter can be synthesized in terms of complex (or inhomogeneous) plane waves. Indeed, the study of reflection and diffraction of Gaussian beams is not only of importance in optics, but it is also important in the analysis and design of millimeter (mm) and sub-millimeter (sub mm) wave antenna systems and components. In the last reporting period, it was indicated that a set of approximate and useful closed form solutions were developed for the reflection and transmission of quite general three-dimensional (3-D) astigmatic EM Gaussian beams (GB's) with a view towards developing a GTD-like solution for GB's. That was in turn preceeded by the development of approximate closed form solutions for the near and far zone reflection of 2-D GB's, and for the approximate far-zone diffraction of 2-D GB's by an edge in a perfectly conducting curved screen. During the present reporting period, work has been essentially completed on extending the previous far-zone edge diffraction of 2-D GB's so that it now remains valid in the near zone of the edge. In addition, a solution to the diffraction of a rotationally symmetric GB by an edge in a 3-D curved screen has also been obtained in closed form for the special case when the plane of incidence is lined up with the principal directions on the

surface containing the edge. Additional extensions to include the diffraction of an astigmatic GB by a perfectly conducting edge in an otherwise smooth boundary are in progress.

The development of additional highly useful frequency domain UTD solutions for describing the complex phenomena of the diffraction of waves by edges in material media which are penetrable is continuing. In particular, a new UTD solution has been obtained for the diffraction of an arbitrarily polarized EM plane wave incident obliquely on a perfectly conducting half plane coated identically on both sides by a thin penetrable material. Such UTD solutions are useful in the analysis of radiating systems associated with modern aerospace vehicles which are partially coated with or constructed from complex penetrable materials.

The above developments are described next in slightly more detail.

2. Time-Domain UTD (TD-UTD)

Exact analytical solutions for transient EM radiation and scattering are available for only a very limited number of simple configurations. It is therefore desirable to develop analytical solutions for predicting the transient EM phenomenon associated with realistic radiating configurations which are generally quite complex. Such analytical time domain (TD) solutions would provide useful physical insight into the behavior of transient wave phenomenon in a way which is generally not possible via the conventional numerical inversion of the corresponding frequency domain solution into the time domain. Thus, work was initiated to develop a TD version of the UTD as discussed in the previous JSEP annual report. Such a TD-UTD development would provide a progressing wave picture for transient radiation and scattering that is analogous to the simple ray picture provided by the frequency domain UTD. The development of a TD-UTD is being performed by an analytical inversion of the corresponding frequency domain UTD. Since the UTD is an asymptotic high frequency technique, the corresponding TD-UTD should be valid in the early to intermediate times after the arrival of the wavefronts corresponding to the different frequency domain ray mechanisms. It should also be possible to combine such TD-UTD solutions via a hybrid scheme with the late time solutions which can be obtained from numerical solutions of the governing space-time integral or differential equations.

11

During the present period, the UTD solution for the diffraction by a perfectly-conducting general curved wedge [1] has been transformed analytically to the time domain (TD). This TD-UTD solution for describing the transient diffraction by a general curved wedge is actually a generalization of the TD-UTD solution obtained previously be Veruttipong and Kouyoumjian [6]. It is noted that this TD-UTD wedge diffraction solution allows for both the edge as well as the wedge faces which form the edge to be arbitrarily curved. However, since the surface ray or whispering gallery mode effects are not present in the UTD solution for a wedge in [1], the corresponding TD-UTD therefore also does not contain these effects, but they will be included in the future phases of this study. This TD-UTD curved wedge solution is not causal for rays which pass through an odd number of caustics as mentioned in the introduction and also as discussed in the previous annual report. This difficulty arises from the fact that a frequency domain geometrical optics or diffracted ray field undergoes a phase jump of $\pm\frac{\pi}{2}$, for ($e^{\pm j\omega t}$) angular frequencies, whenever it traverses a caustic. As indicated in the previous annual report, a study was initiated to address this difficulty of non-causality, and some steps to overcome this limitation have been achieved. In particular, it was examined as to when to properly turn on the time domain response (which is otherwise non-causal) through an analysis of a useful test example which happened to be a two-dimensional (2-D) concave parabolic reflector illuminated on axis by an impulsive plane wave. That example was solved by the TD-UTD and compared with a solution based on a valid physical optics (PO) approximation which could be inverted exactly into the time domain (TD). This TD-PO solution provided information on a procedure for converting the non-causal TD-UTD result (which resulted when the observer was located on the reflector axis beyond the focus (caustic)) into a causal one. The resulting corrected TD-UTD solution contains a precursor that exists prior to the arrival of the UTD wavefront for the reflected field component, which has passed through the focus; however this precursor is now causal. It remains therefore to arrive at a general rule to determine the turn on time for the precursor so that it remains causal in other more general situations where a transient wavefront has passed through an odd number of smooth caustics of the corresponding rays in the frequency domain. With that view in mind, some additional configurations were analyzed during the present period. In particular, an extension of the transient analysis of

12

the above mentioned 2-D concave parabolic reflector was performed to deal with a more general 2-D curved reflector-flat strip combination. In this combination, a flat 2-D strip of finite width was attached to one of the edges of the previous 2-D concave parabola. The angle of the flat strip was allowed to vary and in one case it was made to provide a smooth extension of the parabola along its tangent at the point of attachment. In the latter case, the slope across the parabola-strip junction is made continuous, but the radius of curvature is discontinuous there. For any other angle of the strip, the slope across the parabola-strip junction exhibits a discontinuity. The example of a combined concave parabola-flat strip geometry was chosen as it is much closer to a more general situation (as which might occur on a complex object which is built up in terms of such combined surfaces) than is possible with just a single parabolic contour of finite width. According to the procedure developed to make the TD-UTD solution for the transient scattering by a single 2-D concave parabola causal, it was predicted that the addition of the flat strip to the concave parabola would not change the turn on time of the causal precursor for the reflected wavefront, in the corrected TD-UTD solution for this case, from what it would be for just the concave parabola case without the flat strip attachment. Indeed, this prediction was completely verified by a TD-PO solution for the concave parabola-flat strip combination thus lending further support to this procedure for making the TD-UTD causal. Additional tests are in progress, and a numerical finite difference time domain (FDTD) solution is being sought to provide a more rigorous reference solution than the TD-PO solution, and thereby more clearly demonstrate the validity of the proposed procedure for keeping the TD-UTD solutions causal.

The UTD can be patched up in the regions of caustics of edge diffracted rays, where it fails, via the equivalent current method (ECM) [7, 8] or the incremental theory of diffraction (ITD) [9]. Outside the caustic regions, the ECM and ITD automatically reduce to the UTD. An alternative TD-UTD solution which remains causal through caustics of edge diffracted rays is therefore being constructed by developing a time domain version of ECM, or ITD, which can henceforth be referred to as TD-ECM, or TD-ITD, respectively. In particular, the ECM based solution of Chiang and Marhefka [10] was converted analytically into the time domain in closed form for the case of an impulse plane wave illumination of a perfectly conducting circular disc. This TD-ECM solution is causal and it compares well in the caustic

region with the corresponding TD-PO solution which has also been developed. Furthermore, the TD-ECM approach is seen to furnish the same information as that indicated by the previous procedure to make the TD-UTD causal. Future work will involve the development of TD-UTD and TD-ECM/ITD approaches to deal with more general situations such as those required to deal with the transient response of complex radiating objects.

3. Diffraction by Thin Material Edges/Junctions and Coated Conducting Edges

As reported last year, two very important developments in this area of research are the use of generalized impedance (GIBC) and resistive (GRBC) boundary conditions to replace the material scatterers and secondly, the development of generalized junction or edge conditions. The GIBC are used to model conducting surfaces coated with thin materials; whereas, the GRBC are used to model thin material slabs. The generalized edge/junction conditions, which were obtained by means of a quasi-static analysis, are necessary to assure uniqueness of the solutions. Furthermore, another significant property of these newly developed edge/junction conditions is that they yield solutions that satisfy the reciprocity principle. Once the material scatterer is replaced by a GIBC/GRBC, the scattering problem becomes a mixed boundary value problem. Two functional analytic methods, namely, the Wiener-Hopf and the Maliuzhinets methods have been used to solve for the fields scattered by a variety of geometries. The results obtained last year were published in two journals [11, 12] and also were part of a PhD dissertation. A case not considered before, namely, the scattering by a coated perfect electric conducting (PEC) half-plane illuminated by an obliquely incident plane wave, was considered this year. In this geometry, the coating is the same on both sides of the PEC. The results of this study were submitted for publication to a technical journal [13]. Currently, the more general case of different coatings on both sides of the PEC half-plane is being considered. This latter geometry is more suitable for the Maliuzhinets technique because the Wiener-Hopf scheme would yield matrices that need to be factorized. At the present time only a very limited class of matrices can be factorized. The Maliuzhinets-based analysis in conjunction with a GIBC of order $O(t)$ will yield nonunique

14

solutions; however, the previously developed generalized edge conditions will allow us to completely solve this mixed boundary value problem.

The results obtained in this topic of research are now being used in a variety of applications. For example, the Maliuzhinets-based results for an impedance wedge have been extended to treat the scattering by an impedance wedge with a resistive card attached to the edge of the wedge [14]. The resistivity of the card can vary in a piecewise constant fashion if multiple interactions are included to take into account the discontinuity of the resistivity at a number of discrete points. These results have been used in conjunction with a synthesis algorithm to design a profile of the resistivity to obtain a desired frequency response of a PEC half-plane with a resistive card attached to its edge [15]. One case that was considered was a Chebyshev response where five and nine section resistive cards were used. Some of this work was funded by agencies other than JSEP, and there is the possibility of funding by private industry to use these results in other areas such as antenna design.

Another application of the above research is an ongoing effort to obtain a hybrid solution to the scattering by an impedance wedge with a material body of arbitrary shape and with very general electrical properties attached to or in the vicinity of the wedge apex. Solutions obtained in the past under this funding are being used to obtain a numerically efficient two dimensional Green's function. This work is described in more detail in the section of Hybrid Studies in this report. A third possible application of the research conducted in this area that may be explored in the near future is the extension of the results obtained in the frequency domain to the time domain. However, since the final results in the frequency domain are valid for high frequencies, the time domain results will be valid for early to intermediate times.

As far as the development of new GIBC/GRBC is concerned, last year it was reported that new boundary conditions were developed for planar chiral slabs. Although these boundary conditions are exact, they cannot be easily used to solve boundary value problems. Thus, it is necessary to obtain approximate expressions that are suitable for this purpose. There are a variety of approximations that can be made depending on the accuracy that is desired. In this past year, several approximate expressions for these newly developed GIBC/GRBC have been developed. To access the accuracy of these new expressions, the fields reflected

15

and transmitted by a chiral slab were calculated with these approximate GIBC/GRBC and compared with the exact results.

4. Extensions of UTD

It is worthwhile to continue to extend the established power and versatility of the UTD to deal with a wider variety of complex radiating configurations than is currently possible. This can be accomplished by developing solutions to appropriate and useful canonical problems for describing additional diffraction phenomena. Furthermore, continued developments in the UTD can also be crucial to the development of new time domain UTD (TD-UTD) solutions as well as to the development of hybrid methods which combine high frequency UTD with low frequency numerical techniques.

During the present period, a new canonical UTD solution has been developed to predict the radiation by a magnetic point current source (which can be simulated by an infinitesimal slot antenna) on an elongated smooth perfectly-conducting convex surface when the observer is located within the paraxial region. This new result extends the previously developed UTD solution for antennas on a perfectly-conducting convex surface which was not valid within the paraxial region [3]. Furthermore, the paraxial solution properly recovers the previously developed UTD solution of [3] when the observation point moves outside the paraxial region. The UTD transition function which keeps the new radiation solution valid within the paraxial region is related to the parabolic cylinder function. This paraxial UTD radiation solution will be able to predict the radiation within paraxial region of conformal antennas and antenna arrays on smooth, perfectly-conducting elongated convex surfaces. In addition, it will be very useful to the development of a hybrid MM-UTD solution (see more discussion in the Hybrid Studies work unit) for aircraft/missile shapes which would also remain valid within the paraxial regions of such shapes. A hybrid solution currently developed for such shapes is valid only outside the paraxial zone. This paraxial UTD radiation solution will be tested for its accuracy by comparison with some appropriate measurement such as for an antenna on an elongated spheroid (or ellipsoid) since it does not appear to be easy to find another independent solution as a check for this relatively general electrically large spheroidal (or ellipsoidal) configuration. An extension to this paraxial UTD solution is being investigated

16

next. The latter important extension will allow one to predict the radiation within the paraxial zone of antennas on an elongated smooth convex surface but with an end cap to simulate, for example, the bulkhead in the nose of an aircraft where it is joined to a transparent radome (which encloses an antenna assembly attached to the bulkhead).

Another useful extension to the UTD which has been achieved recently is the diffraction of an inhomogeneous plane wave by an impedance wedge. This UTD solution is expected to be useful, for example, in the analysis of the diffraction by a highly conducting wedge type inhomogeneities in a lossy medium, as might occur in underground remote sensing with EM waves. In particular, this solution indicates that the shadow zones are quite different than those produced by a real (homogeneous) plane wave when it illuminates an impenetrable wedge in a loss free medium. This UTD solution for the diffraction of an inhomogeneous plane wave by an impedance wedge is also useful to the study of the diffraction of a Gaussian beam (GB) by an edge since a GB can be synthesized in terms of a spectrum of homogeneous and inhomogeneous plane waves.

The study of the reflection and diffraction of general three-dimensional (3-D) Gaussian beams (GB's) from curved perfectly conducting surfaces with edges is in progress. Such a study is useful since there are some situations where ray techniques such as the GTD/UTD, as versatile as they are, may become cumbersome or inapplicable. Examples of such situations may deal with the analysis/design of large reflectors with an array feed, or phased arrays, especially in focal regions, and in the radiation and propagation of millimeter and submillimeter waves through radiating systems or open or closed waveguide systems, etc. The idea here is to attempt to develop a theory for propagation reflection and diffraction of GB's which may in some sense be viewed as a GTD for GB's. A set of approximate and useful closed form solutions were developed for the reflection and transmission of 3-D astigmatic GB's; this was reported in the previous annual report. Prior to that, approximate but accurate solutions were also developed for the reflection and edge diffraction of 2-D GB's; the latter edge diffraction result was valid only in the far zone. During the present period, work has essentially been completed on the extension of the previous far zone solution for the edge diffraction by a 2-D GB so that it now remains valid in the near zone just as the 2-D GB reflection solution does. Furthermore, the diffraction of rotationally symmetric GB's by

an edge in a 3-D curved screen has also been obtained in closed form for the special case when the plane of incidence is lined up with the principal directions on the surface containing the edge. The diffraction of 2-D and 3-D GB's is analyzed by appropriately evaluating the radiation integral over the high frequency estimate of the current induced on the diffracting surface by these beams. The next step will be to generalize these results so that they remain valid for general 3-D astigmatic EM GB's, and following that, these general results will be employed to demonstrate their usefulness in analyzing/synthesizing large reflectors and their feed arrays as well as a host of other interesting radiating configurations via GB's.

References

[1] R.G. Kouyoumjian and P.II. Pathak, "A Uniform Geometrical Theory of Diffraction for an Edge in a Perfectly Conducting Surface," *Proc. of the IEEE*, Vol. 62, pp. 1448-1461, November 1974.

[2] P.H. Pathak, W.D. Burnside and R.J. Marhefka, "A Uniform GTD Analysis of the Scattering of Electromagnetic Waves by a Smooth Convex Surface," *IEEE Trans. on Antennas and Propagation*, Vol. AP-28, pp. 631-642, September 1980.

[3] P.H. Pathak, N.N. Wang, W.D. Burnside and R.G. Kouyoumjian, "A Uniform GTD Solution for the Radiation from Sources on a Convex Surface," *IEEE Trans. on Antennas and Propagation*, Vol. AP-29, pp. 609-622, July 1981.

[4] P.H. Pathak and N.N. Wang, "Ray Analysis of Mutual Coupling between Antennas on a Convex Surface," *IEEE Trans. on Antennas and Propagation*, Vol. AP-29, pp. 911-922, November 1981.

[5] J.B. Keller, "Geometrical Theory of Diffraction," *J. Opt. Soc. Am.*, Vol. 52, pp. 116-130, 1962.

[6] T.W. Veruttipong, "Time Domain Version of the Uniform GTD," *IEEE Trans on Antennas and Propagation*, Vol. AP-38, pp. 1757-1764, November 1990.

[7] C.E. Ryan, Jr. and Leon Peters, Jr., "Correction to 'Evaluation of Edge-Diffracted Fields including Equivalent Currents for the Caustic Region'," *IEEE Trans. on Antennas and Propagation*, Vol. AP-18, p. 275, March 1970.

[8] C.E. Ryan, Jr. and Leon Peters, Jr., "Evaluation of Edge-Diffracted Fields including Equivalent Currents for the Caustic Region," *IEEE Trans. on Antennas and Propagation*, Vol. AP-17, pp. 292-299, May 1969.

[9] R. Tiberio and S. Maci, "A Spectral Incremental Diffraction Coefficient," URSI Digest, International AP-S/URSI Meeting, Chicago, Illinois, p. 498, July 18-25, 1992.

[10] K.C. Chiang and R.J. Marhefka, "Bistatic Scattering from a Finite Circular Cylinder," The Ohio State University, ElectroScience Laboratory, Technical Report 714614-4, July 1984.

[11] H.C. Ly, R.G. Rojas and P.H. Pathak, "EM Plane Wave Diffraction by a Planar Junction of Two Thin Material Half-Planes - Oblique Incidence," *IEEE Trans. on Antennas and Propagation*, Vol. 41, pp. 429–441, April 1993.

[12] H.C. Ly and R.G. Rojas, "Analysis of Diffraction by Material Discontinuities in Thin Material Coated Planar Surfaces Based on Maliuzhinets Method," *Radio Science*, Vol. 28, pp. 281–297, May–June 1993.

[13] H.C. Ly and R.G. Rojas, "EM Plane Wave Diffraction by a Material Coated Perfectly Conducting Half-Plane (Oblique Incidence)," submitted for publication, *Microwave and Optical Technology Letters*.

[14] R.G. Rojas and M.F. Otero, "Scattering by a Resistive Strip Attached to an Impedance Wedge," *J. Electromagnetic Waves and Applications (JEWA)*, Vol. 7, No. 3, pp. 373-402, 1993.

[15] M.F. Otero and R.G. Rojas, "Synthesis of the Frequency Response of an Inhomogeneous Resistive Strip," to be submitted to *Annales of Telecommunications*, special issue on RCS of complex objects.

5. Diffraction Studies — JSEP Publications

Published refereed journal papers:

1. H.C. Ly, R.G. Rojas and P.H. Pathak, "EM Plane Wave Diffraction by a Planar Junction of Two Thin Material Half-Planes — Oblique Incidence," *IEEE Transactions on Antennas and Propagation*, Vol. 41, No. 4, pp. 429–441, April 1993.

2. H.C. Ly and R.G. Rojas, "Analysis of Diffraction by Material Discontinuities in Thin Material Coated Planar Surfaces based on Maliuzhnets' Method," *Radio Science*, Vol. 28, pp. 281–297, May–June 1993.

3. G.A. Somers, "A Proof of the Woodward-Lawson Sampling Method for a Finite Linear Array," *Radio Science*, pp. 481–485, July–August 1993.

4. R.G. Rojas and M. Otero, "Scattering by a Resistive Strip Attached to an Impedance Wedge," *Journal of Electromagnetic Waves and Applications (JEWA)*, Vol. 7, No. 3, pp. 373-402, 1993.

Accepted refereed journal papers:

1. G.A. Somers and P.H. Pathak, "Efficient Numerical and Closed Form Asymptotic Representations of the Dyadic Aperture Green's Function for Material Coated Ground Planes," *Radio Science.*

Oral presentations:

1. SHORT COURSE: R.G. Rojas, "Prediction of Mounted Antenna's Radiation Pattern using the GTD/UTD Approach," invited short course at PT. Industri Peswat Terbang Nusantara (IPTN), Banbung, Indonesia, November 1992.

2. P.H. Pathak, "A Review of Some Asymptotic HF Methods with Applications to Electromagnetic Radiation and Scattering," invited IEEE AP-S distinguished lecture, IEEE AP-S/MTT chapter in Atlanta, Georgia, January 27, 1993.

3. H.T. Anastassiu and P.H. Pathak, "High Frequency Analysis of Gaussian Beam Scattering by a Parabolic Surface Containing an Edge," International IEEE AP-S and National URSI meeting in Ann Arbor, Michigan, June 28–July 2, 1993.

4. G.A. Somers and P.H. Pathak, "An Asymptotic Closed Form Aperture Green's Function with Applications to Radiation and Scattering by Slots in Material Coated Ground Planes," International IEEE AP-S and National URSI meeting in Ann Arbor, Michigan, June 28–July 2, 1993.

5. H.T. Anastassiu and P.H. Pathak, "A Simple Gaussian Beam Analysis of the Fields Radiated by Two-Dimensional Paraboloid Reflector Antennas Illuminated by a Feed Array," International IEEE AP-S and National URSI meeting in Ann Arbor, Michigan, June 28–July 2, 1993.

6. P.H. Pathak, "Some Recent Accomplishments and Future Directions in the Area of High Frequency Techniques," invited lecture, XXIVth General Assembly of URSI, Kyoto, JAPAN, August 25–September 3, 1993.

IV. INTEGRAL EQUATION ANALYSIS OF ARTIFICIAL MEDIA

Researchers:

E.H. Newman, Professor   (Phone: 614/292-4999)
M. Peters, Graduate Research Associate   (Phone: 614/294-9273)

1. Introduction

This section will summarize our work in integral equation studies from September 1992 to September 1993. In overview, our recent research has centered on integral equation and method of moments (MM) solutions for artificial media. In particular, we have developed a flexible and accurate integral equation and method of moments procedure for determining the effective permittivity and permeability of artificial media. Previously the method has been applied to relatively simple artificial media composed of 2D dielectric rods, short perfectly conducting dipoles, and small lossy dielectric spheres [1, 10, 3]. During the past year we have extended these techniques to artificial media constructed from thin conducting or dielectric rods of essentially arbitrary configuration (i.e. straight rods, loops, crosses, tee's etc.) [4, 5]. In particular, this has necessitated the computation of the effective *dyadic* permittivity and permeability of anisotropic artificial media.

As illustrated in Figure 1, an artificial medium is created by suspending a large number of small scatterers, such as spheres, discs, dipoles, etc., in some host or background medium. For computational convenience, the small scatterers are assumed to be identical and on a periodic lattice. An electromagnetic field in this artificial medium will induce currents to flow on or in the small scatterers. In this case, each of the scatterers can be viewed as having a small electric and/or magnetic current moment, and thus the array can be viewed as having some net electric dipole polarization P per unit volume and/or magnetic dipole polarization M per unit volume. Essentially, the macroscopic scatterers in the artificial medium are equivalent to the microscopic current moments produced by atoms and molecules in a real medium.
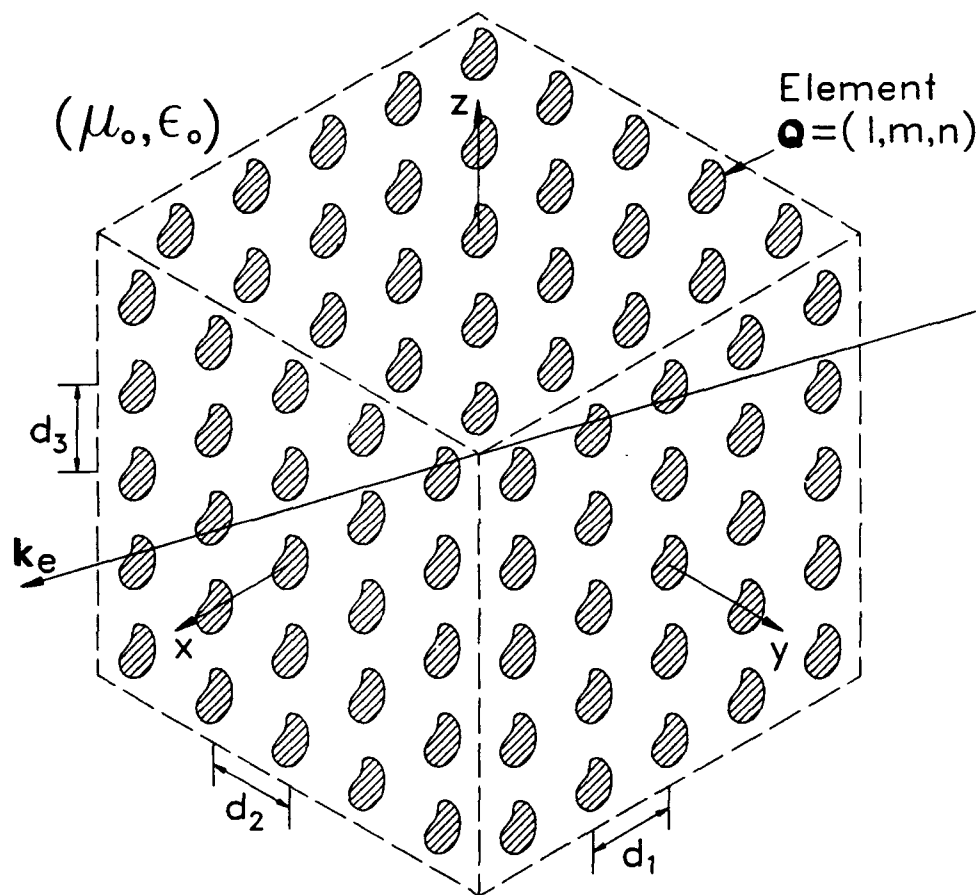
Figure 1: A triple infinite periodic array of scatterers representing an artificial dielectric.

In the artificial medium, the electromagnetic field vectors are related by

$$\mathbf{D}^0 = \epsilon_0 \mathbf{E}^0 + \mathbf{P}^0 = \epsilon_0 \mathbf{E}^0 + \epsilon_0 \bar{\chi}^e \cdot \mathbf{E}^0 = \bar{\epsilon}_r \cdot \mathbf{E}^0 \qquad (1)$$

$$\mathbf{B}^0 = \mu_0(\mathbf{H}^0 + \mathbf{M}^0) = \mu_0(\mathbf{H}^0 + \bar{\chi}^m \cdot \mathbf{H}^0) = \bar{\mu}_e \cdot \mathbf{H}^0 \qquad (2)$$

where (μ_0, ϵ_0) are the permeability and permittivity of the homogeneous isotropic background media, $\bar{\chi}^e$ and $\bar{\chi}^m$ are the dimensionless dyadic effective electric and magnetic susceptibilities, $(\bar{\mu}_e, \bar{\epsilon}_e)$ are the effective dyadic permeability and permittivity of the anisotropic artificial media, and the ^{0} superscripts indicate that the quantity has been computed for or averaged over the center cell of the periodic lattice of the artificial media. The main purpose of our research is to determine the effective permittivity and permeability of the artificial medium as a function of:

1. the size, shape, and material composition of the small scatterers.

2. the density of the small scatterers

3. the frequency

This will permit the designing or "engineering" of an artificial medium to have some prescribed $(\bar{\mu}_c, \bar{\epsilon}_c)$. The artificial media model also appears to be applicable to the modeling of composite materials (see dielectric weave example below), battlefield combat induced atmospheric obscurants, such as chaff, rain, smoke, etc. [6] (see lossy dipole example below), and absorbers. Another potentially interesting application is the inverse problem. That is given the effective parameters of an artificial medium (say by measurements) what can be deduced concerning the properties of the small scatterers.

2. Overview of the Method

At present we are considering an artificial medium composed of thin conducting or dielectric rods of essentially arbitrary shape in a periodic lattice. It is assumed that a plane wave is propagating in the artificial medium in a given direction. However, since the effective permittivity and permeability of the artificial medium are unknown, the phase constant(s) k_c of this wave is unknown. The objective of the solution is to find this phase constant, from which $(\bar{\mu}_c, \bar{\epsilon}_e)$ can be deduced.

Our method of solution is based upon an essentially exact full wave analysis. The first step is to use the volume equivalence theorem to replace the array of small scatterers by the background medium and unknown equivalent electric polarization currents. These unknown polarization currents can be formulated as the solution to a volume integral equation. This integral equation is exact and includes all interactions between the elements in the triple infinite periodic array. However, due to the periodicity of the problem, the only unknown is the current in the center element, and the volume integral equation need only be enforced in the center element.

The integral equation is solved by a numerical technique known as the method of moments (MM). Essentially, the unknown current on the center element is expanded in terms of N basis or expansion functions, and the integral equation is enforced for N weighting or testing functions. The result is that the integral equation is reduced to an order N matrix equation

$$[Z(k_r)]I = V \tag{3}$$

where $[Z]$ is the order N impedance matrix, V is the length N excitation vector, and I is the length N current vector which holds the coefficients in the original expansion for the current. As is emphasized in Equation (3), the elements in impedance matrix are a function of the unknown phase constant k_c.

Since a plane wave is a solution of Maxwell's *source free* equations, we seek a solution of Equation (3) for which the excitation vector $V = 0$, i.e.,

$$[Z(k_c)]I = 0. \tag{4}$$

Such solutions can be termed the normal, natural, or eigenfunction modes of the artificial medium, and are only possible if the determinant of the impedance matrix is zero, i.e.,

$$\det|Z(k_c)| = 0. \tag{5}$$

Equation (5) must now be solved in an iterative fashion for k_c. Once k_c is known, $(\bar{\mu}_c, \bar{\epsilon}_r)$ can be found. For the simple case in which the artificial medium is an isotropic non magnetic medium, then

$$k_c = \omega\sqrt{\mu_0\epsilon_c} \rightarrow \epsilon_c = \frac{k_c^2}{\omega^2\mu_0}. \tag{6}$$

For anisotropic artificial media, more complex procedures are required to deduce the dyadic effective parameters [4, 5].

3.   Example Results

The insert in Figure 2 shows an artificial medium formed by a weave of dielectric wires of relative permittivity 10 and loss tangents of 0 and 1. This dielectric weave is a model for a composite material. The figure shows the effective relative permittivity of the artificial medium as a function of the weave size L/λ_0. The relative effective permittivity of the weave is about 1.7. For the wires with a loss tangent of 1, the effective loss tangent of the weave is about 0.5.

One application for artificial media is in the design of chaff. For example, consider the design of a chaff cloud composed of lossy dipoles, and designed to provide maximum attenuation of an EM wave propagating through it. The question is what loss tangent for the dipoles will maximize the effective loss tangent of the artificial media (and thus maximize the attenuation of the EM wave). The insert in Figure 3 shows an artificial medium composed of lossy thin wire dipoles of length $0.2\lambda_0$. The figure shows the effective permittivity and loss tangent of the artificial medium as a function of the loss tangent of the dipoles. It is seen that a dipole loss tangent of about 600 will provide a maximum effective loss tangent of about 0.7 for the artificial medium.

Dielectric Weave Perm.
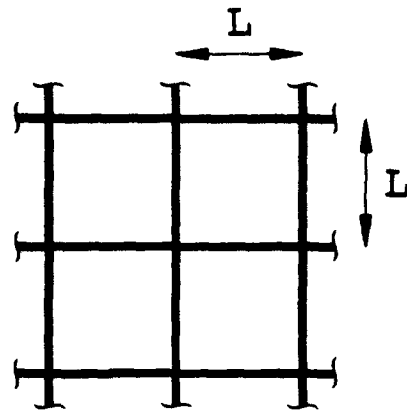
$$N = 7$$
MM Modes

$d_x = d_y = L$
$d_z = 0.4L$
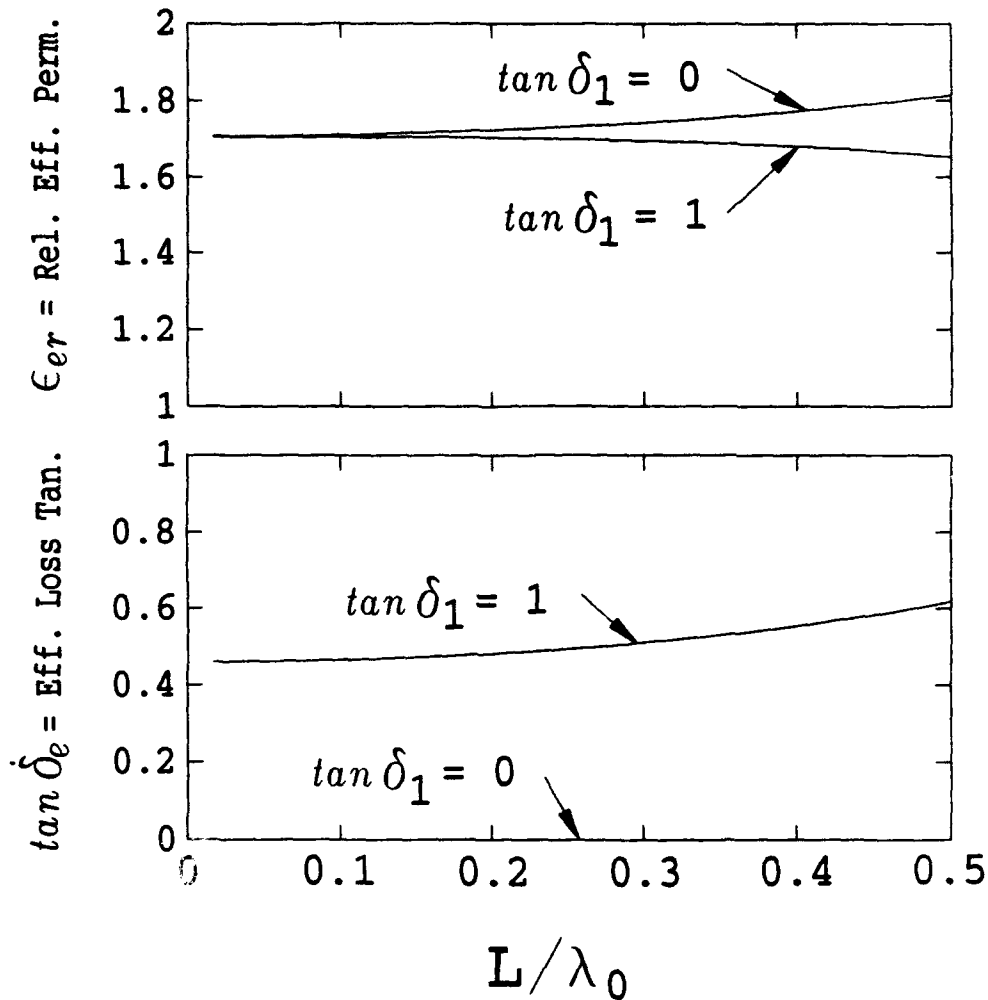$a = 0.2L$
$\epsilon_1 = 10$
$tan\,\delta_1 = 0, 1$

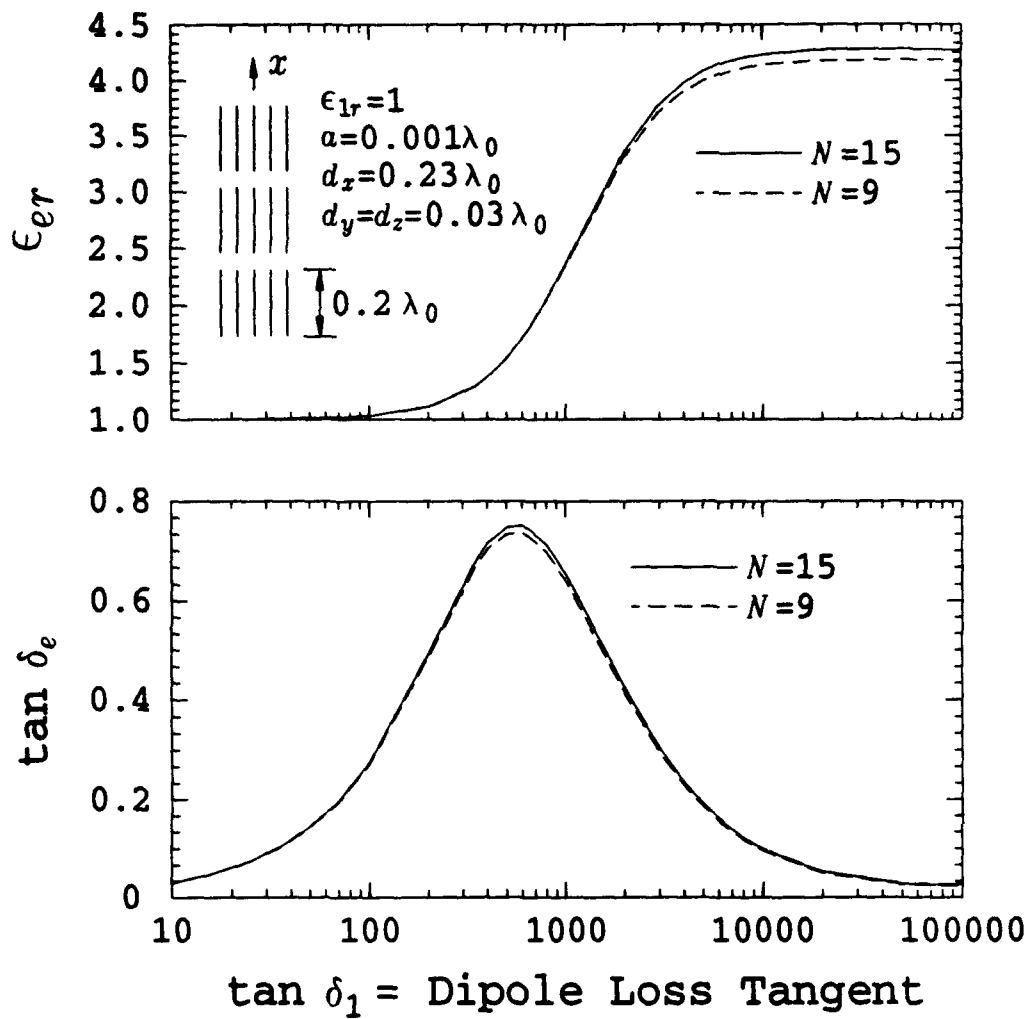Figure 2: A dielectric weave composite material modeled as an artificial dielectric.

Figure 3: An artificial media composed of lossy dipoles modeling a chaff cloud.

References

[1] J.L. Blanchard, "Integral Equation Analysis of Artificial Dielectrics", PhD dissertation, Ohio State University, Dept. of Mathematics, 1991.

[2] J.L. Blanchard, E.H. Newman, and M.E. Peters "Integral Equation Analysis of Artificial Media," IEEE Trans. on Antennas and Propagation, accepted for publication.

[3] M.E. Peters and E.H. Newman, "Analysis of an Artificial Dielectric Composed of Small Dielectric Spheres," IEEE Trans. on Antennas and Propagation, submitted for publication.

[4] E.H. Newman and M.E. Peters, "Integral Equation Analysis of Artificial Media," 1993 IEEE Antennas and Propagation Society and Radio Science Meeting, Ann Arbor, Michigan, June 28 - July 2 1993.

[5] M.E. Peters, "Method of Moments Analysis of Artificial Media Composed of Thin Conductive or Dielectric Wire Objects," PhD Dissertation, Ohio State University, Dept. of Electrical Engineering, in progress.

[6] E.H. Newman and M.E. Peters, "Integral Equation Analysis of Artificial Media," 1993 Workshop on the Electromagnetics of Combat-Induced Atmospheric Obscurants, El Paso, Texas, Nov. 2-4 1993.

4. Integral Equation Studies — JSEP Publications

Published refereed journal papers:

1. N. Wang and L. Peters, Jr., "Scattering by Thin Wire Loaded with a Ferrite Ring," *IEEE Transactions on Antennas and Propagation*, Vol. 41, No. 5, pp. 694–697, May 1993.

Accepted refereed journal papers:

1. J.L. Blanchard, E.H. Newman and M.E. Peters, "Integral Equation Analysis of Artificial Media," *IEEE Transactions on Antennas and Propagation*.

2. R. Torres and E.H. Newman, "Integral Equation Analysis of a Sheet Impedance Coated Window Slot Antenna," *IEEE Transactions on Antennas and Propagation*.

V. FINITE ELEMENT TECHNIQUES

Researchers:

R. Lee, Assistant Professor	(Phone: 614/292-1433)
U. Pekel, Graduate Research Associate	(Phone: 614/292-7981)
Y. S. Choi-Grogan, Graduate Research Associate	(Phone: 614/292-7981)
J. Jevtic, Graduate Research Associate	(Phone: 614/294-9280)
T. Barkdoll, Graduate Research Associate	(Phone: 614/292-7981)

1. Introduction

The research for Work Unit III in this past year has been to continue some of the research work done the previous year. Also, we have begun work on several new and promising research topics. All of the research in this work unit has been centered on the development of numerical techniques which either improve the accuracy or the efficiency of the finite element method (FEM) for electromagnetics.

There has been two major thrusts of the research this year. One is the development and analysis of new boundary truncation techniques for electromagnetic propagation and scattering problems in unbounded regions. In the previous two year's reports, we provided a short discussion of the development of the bymoment method for electromagnetic scattering from three-dimensional (3-D) objects in free space. This work is now complete, and we will show results for this method. Approximately one and a half years ago, a new boundary truncation technique called the measured equation of invariance (MEI) was introduced by Dr. Ken Mei. Based on the initial presentation of the method, we felt that this method had the potential to overcome some of the weaknesses of the bymoment method. Over the past year, the majority of our research efforts on boundary truncation methods has been concentrated on the development and analysis of the MEI. The results of this work will be discussed in this report.

The second major area of research is the continuing development of the partitioning technique that was discussed in last year's report. In the partitioning method, the computation domain is decomposed into subdomains. By decoupling the subdomains, we are able to solve

the problem in each subdomain very efficiently. The final coupling of the subdomains is also done in a very efficient manner. One of the other advantages of this partitioning method is that it can be easily and efficiently implemented onto massively parallel computers. The performance on a parallel computer will be discussed in this report.

2. The Bymoment Method for 3-D Scattering Problems

The bymoment method is a rigorous boundary truncation technique for the FEM. Over the past two years, we have been developing the bymoment method for three-dimensional anal ysis, based on the two dimensional formulation [1]. As with many methods, the extension to three dimensions is not straightforward. The details of the derivation for the 3-D bymoment method was presented in the annual JSEP report in 1991, and one should refer to that report when considering the details discussed here. In that report, we chose to use a vector field formulation for the FEM analysis, while we expanded the solution on the mesh boundary in terms of two scalar potentials. By using two scalar potentials rather than a vector field to represent the solution on the boundary, we are able to reduce the number of unknowns on the boundary by 1/3. At the time of the report in 1991, we were unsure of the type of expansion and testing functions that would be used for the bymoment method. In this report, we describe the expansion and testing functions and validate the method on several problems.

The accuracy and efficiency of the bymoment formulation is strongly dependent on the choice of expansion functions used to represent two z-directed Hertz vector potentials on the outer artificial boundary surface S where the finite element mesh is truncated. Two plausible choices for the expansion functions are the spherical harmonics and the solutions to a multipole expansion on an artificial surface which is enclosed by the mesh boundary surface S. The multipole expansion has reportedly been successfully applied in integral equation methods [2] In order to describe the bymoment method technique, the relevant steps are shown for the case where the expansion functions are assumed to be spherical harmonics. For the special case in which the scattering object has a spherical geometry, this choice is the most natural one. For the case in which the more general multipole expansion functions are employed, the resulting expressions will be conceptually very similar to the

ones that are obtained when spherical harmonics are used. The two Hertz vector potentials can be written on the surface S as

$$\Pi_e = \sum_{n=0}^{N} \sum_{m=0}^{n} a_{mn}^{e,o} \psi_{mn}^{e,o}\left(k_0 \overline{R}\right) \ , \ \ \Pi_m = \sum_{n=0}^{N} \sum_{m=0}^{n} b_{mn}^{e,o} \psi_{mn}^{e,o}\left(k_0 \overline{R}\right)$$

$$\overline{\Pi}_e = \hat{z}\,\Pi_e \ , \ \ \overline{\Pi}_m = \hat{z}\,\Pi_m \ , \ \ k_0 = \omega\sqrt{\mu_0 \epsilon_0} \tag{7}$$

where $\{a_{mn}^{e,o}\}$ and $\{b_{mn}^{e,o}\}$ denote two sets of coefficients to be determined by the "coupling procedure" on the artificial boundary surface S' shown in Figure 4; μ_0 and ϵ_0 are the permeability and the permittivity of free-space, respectively; k_0 is the corresponding free-space wave number, and the scalar expansion functions $\psi_{mn}^{e,o}\left(k_0\overline{R}\right)$ are given for the case of spherical harmonics by:

$$\psi_{mn}^{e,o}\left(k_0\overline{R}\right) = \left\{ j_n\left(k_0 r\right) \ , \ h_n^{(2)}\left(k_0 r\right)\right\} P_n^m\left(\cos\theta\right)\{\ \cos m\phi \ , \ \sin m\phi\ \} \tag{8}$$

In the above expressions, the superscripts "e" and "o" denote even and odd modes, respectively, while the j_n and $h_n^{(2)}$ functions represent the spherical Bessel functions and the spherical Hankel functions of the second kind, respectively, which is in accordance with the $e^{+j\omega t}$ type time-harmonic dependence that is assumed. The P_n^m functions are associated Legendre functions, and the angular variables θ, ϕ lie in the ranges $0 \le \theta \le \pi$ and $0 \le \phi \le 2\pi$, respectively. The radial variable r lies in the range $0 \le r < \infty$, and the integer indices m, n are defined by $0 \le n \le N$ and $0 \le m \le n$, where the integer N controls the number of expansion functions.

The more general class of multipole expansion functions can be defined in a very similar manner as:

$$\psi_{mn}^{e,o}\left(k_0\overline{R}\right) = \tag{9}$$
$$\left\{ j_n\left(k_0\left|\overline{r} - \overline{r}'\right|\right), h_n^{(2)}\left(k_0\left|\overline{r} - \overline{r}'\right|\right)\right\} P_n^m\left(\cos\theta_{mp}\right)\{\cos m\phi_{mp} \ , \ \sin m\phi_{mp}\}$$

where the only difference between these more general multipole expansion functions and the spherical harmonics lies in the fact that the multipole expansion functions are centered at an arbitrary source point $\overline{r}'$, where $\overline{R} = \overline{r} - \overline{r}'$, $0 \le \theta_{mp} \le \pi$, and $0 \le \phi_{mp} \le 2\pi$. It should be mentioned that the "optimum" number and location of these multipoles for a given scattering problem are highly dependent on the geometrical properties of the scattering object, and that
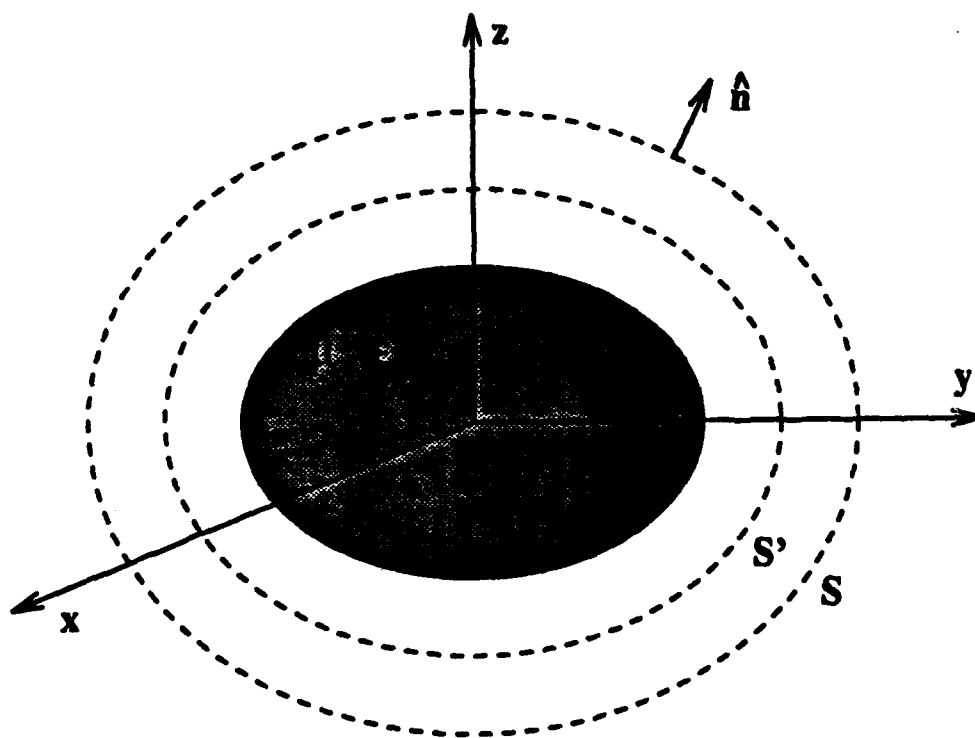
31

Figure 4: The scattering object and the two artificial boundary surfaces S and S'.

an "optimum" approach is presented in the literature [3] which enables the user to obtain an "optimum" number of "numerically complete" multipole expansion functions centered at "optimum" locations for a specific scatterer geometry.

Both of these classes of functions can be applied in order to expand the two Hertz vector potentials in free-space. However, the multipole expansion functions are far more general and versatile in terms of their adaptability to the bymoment method approach. In fact, the spherical harmonics are known to be a special subset of the class of multipole expansion functions. With regard to the choice of spherical Bessel or Hankel functions in order to express the radial variation, it must be noted that one may have to choose the type of function that expresses this variation in accordance with the properties of the incident field. For instance, one must use the spherical Bessel functions (for both classes of expansion functions) in the radial direction if the incident field that illuminates the scatterer is a plane wave. This choice is due to the fact that the series expansion of a plane wave in terms of spherical harmonics is known to contain spherical Bessel functions only.

In order to solve for the coefficients, we formulate the solution at the boundary in terms of an integral equation in which we must choose a set of linearly independent vector testing functions $\overline{\overline{\Phi}}_j^{(E)}$ and $\overline{\overline{\Phi}}_j^{(M)}$, which satisfy both the free-space vector Helmholtz equation and the radiation condition at infinity. The two superscripts (E) and (M) which are associated with these vector testing functions are more of a mathematical nature than of a physical (i.e electric or magnetic) one. Clearly, in the special case where the scattering object is a sphere, the most natural choice for the purpose of generation of these testing functions is the same set of spherical harmonics used above to expand the two Hertz vector potentials. But, the set of multipole expansion functions is an equally suitable and even more general choice for the purpose of generation of the vector testing functions. The general subscript j, which is used in conjunction with the vector testing functions, symbolically represents the the integer subscripts n, m and the superscripts "e" and "o". The symbolic subscript j also accounts for the possibility of having more than one multipole expansion function. If the FEM solutions for the boundary conditions on the surface S have been expanded in terms of spherical Bessel functions in order to express their radial variation, then one must use the spherical Hankel functions in order to express the radial variation of both classes of testing

functions. This choice will ensure that the resulting equations which are obtained at the end of the testing procedure are linearly independent.

However, rather than applying either of the two classes of scalar expansion functions directly, one must first derive the two sets of vector testing functions from the scalar expansion functions, and then apply a vector-based version of Green's theorem on the inner boundary surface S' to the FEM solution for the $\overline{H}$ field and the two vectorial testing functions $\overline{\Phi}_j^{(E)}$ and $\overline{\Phi}_j^{(M)}$. In this work, the vectorial testing functions are derived from the scalar expansion functions $\psi_{kl}^{e,o}$ in the following manner:

$$
\begin{aligned}
\overline{\Phi}_j^{(E)} &= \overline{\Phi}_{kl}^{e,o(E)} = \nabla \times (\hat{z}\psi_{kl}^{e,o}) \\
\overline{\Phi}_j^{(M)} &= \overline{\Phi}_{kl}^{e,o(M)} = \hat{z}\psi_{kl}^{e,o}
\end{aligned}
\tag{10}
$$

where the integer subscripts k, l lie in the ranges given by $0 \leq l \leq N$, $0 \leq k \leq l$, the superscripts "e" and "o" denote even and odd modes, respectively, and N is the particular integer which controls the total number of testing functions. It is clearly seen from these two equations that the superscripts (E) and (M) are assigned to the two vectorial testing functions because of the apparent similarity between the definition of the "electrical/magnetic" testing functions and the definition of the electrical/magnetic boundary condition terms on the surface S. The above definitions of the two vector testing functions ensure a proper balance in the directional properties of the FEM solutions for the $\overline{H}$ field and the testing functions. Furthermore, they also guarantee a balance in the variation of the orders of these two entities. The vector testing functions $\overline{\Phi}_j^{(E)}$ and $\overline{\Phi}_j^{(M)}$ also must satisfy the vector Helmholtz equation because of the way they are derived from the scalar expansion functions $\psi_{kl}^{e,o}$. Thus, one can write the identities:

$$
\begin{aligned}
\nabla^2 \overline{H}^s + k_0^2 \overline{H}^s &= 0 \\
\nabla^2 \overline{\Phi}_j^{(E)} + k_0^2 \overline{\Phi}_j^{(E)} &= 0 \\
\nabla^2 \overline{\Phi}_j^{(M)} + k_0^2 \overline{\Phi}_j^{(M)} &= 0
\end{aligned}
\tag{11}
$$

To validate the bymoment code, we consider the problem of electromagnetic scattering from a perfect electric conducting (PEC) sphere, a lossy dielectric prolate spheroid, and a dielectric cube. The PEC sphere was chosen as the first test geometry since the solution is

known and the computation domain can be limited to a few layers of elements on the surface of the sphere. However, we have found that it is not easy to achieve an accurate finite element solution to the sphere problem. The difficulty does not come from the bymoment method but rather the inability of the FEM to model the geometrical shape of the sphere. The discretization requirements are dominated by the geometry and not the wavelength. Even with a 20-node isoparametric hexahedron, we require 96 elements (678 nodes) to form a single layer elements on the sphere surface in order to obtain excellent results for a sphere with a radius of 0.23 wavelengths. The nodal density is over 100 nodes per wavelength. As we eventually found out, the sphere is one of the most difficult geometries to model due to its curvature. A comparison of the bymoment results (25 spherical harmonic expansion terms) with the Mie series solution is given in Figure 5.

The lossy dielectric prolate spheroid was chosen because numerical solutions are available from codes which compute scattering from bodies of revolution [4]. For the prolate spheroid shown in Figure 6, we obtain the far-field pattern (Figure 7) with the bymoment method and compare it to the results obtained from [4], which we define to be the reference solution. The incident magnetic field is assumed to be polarized in the $-\hat{z}$ direction with the far-field pattern taken in the xy plane. We see that the agreement is very good.

The final geometry is a dielectric cube with sizes of length 0.4 wavelengths (wavelengths in dielectric) and permittivity $\epsilon = 4\epsilon_0$. The far-field pattern is shown in Figure 8. As in the previous geometry, the incident magnetic field is assumed to be polarized in the $-\hat{z}$ direction with the far-field pattern taken in the xy plane. The reference solution is obtained from a method of moments solution [5]. There is reasonable agreement. It should be noted that the reference solution is also obtained from a numerical methods, so it is not clear which one is the correct solution.

3. The Measured Equation of Invariance

The finite element method has always been handicapped in the modeling of electromagnetic phenomena because of its inability to both accurately and efficiently simulate the radiation condition. Recently, the measured equation of invariance (MEI) [6] has been proposed as a rigorous local method for modeling perfectly conducting cylinders. It is based on the
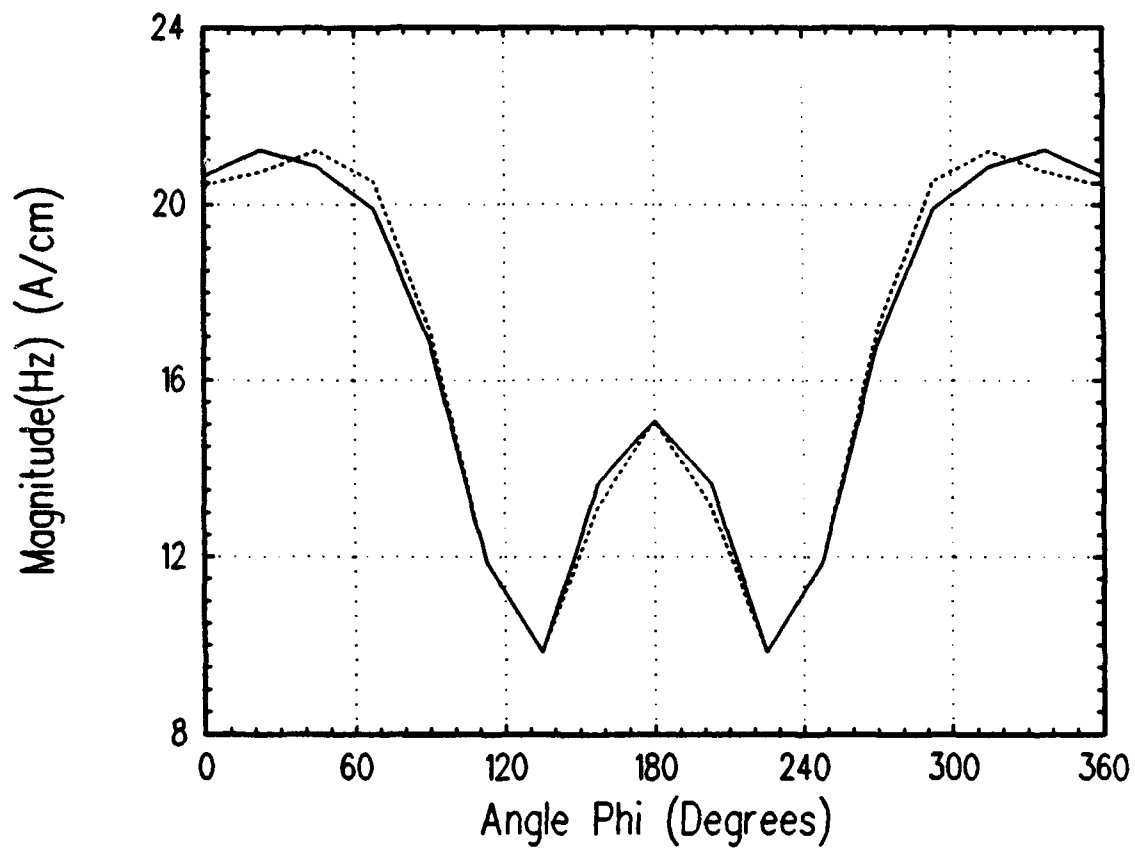
Figure 5: The variation of the calculated (solid line) and exact (dotted line) magnitude of H_z along the circumference of the conducting sphere in the xy-plane.
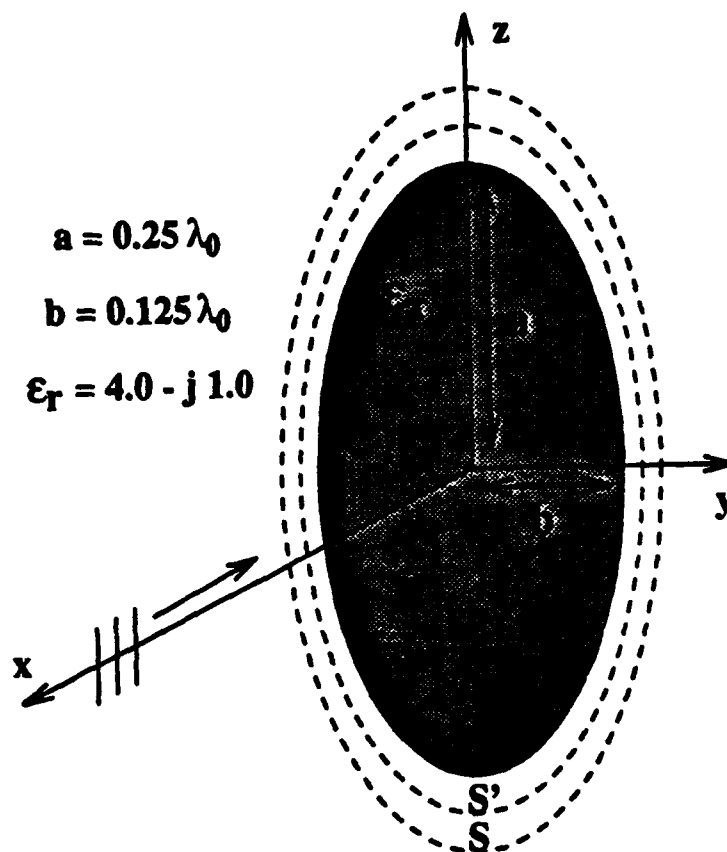
Figure 6: A lossy dielectric prolate spheroid in free-space with an axis ratio of 2:1 and $\epsilon_r = 4.0 - j1.0$.

Figure 7: The variation of the calculated (solid line) and reference (dotted line) magnitude of the normalized far-zone pattern in the xy-plane (E-plane) with a $(-z)$-directed incident magnetic field.

38

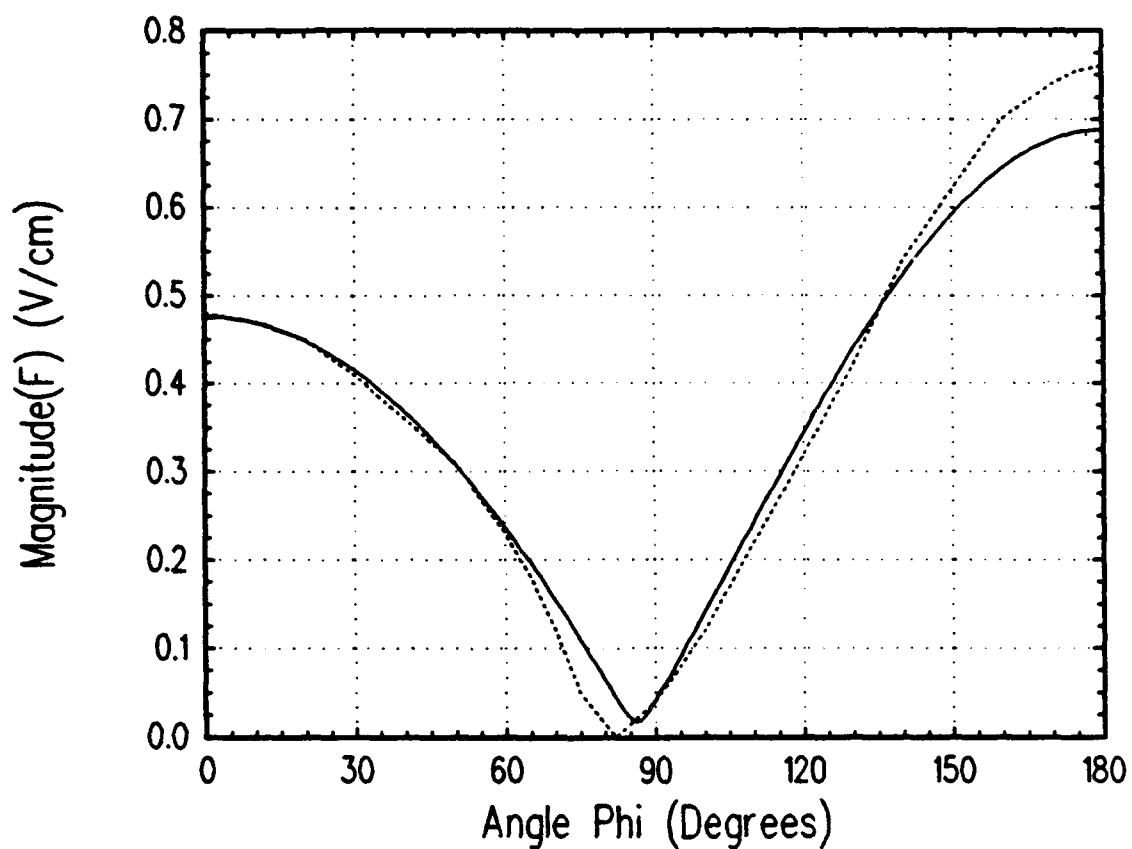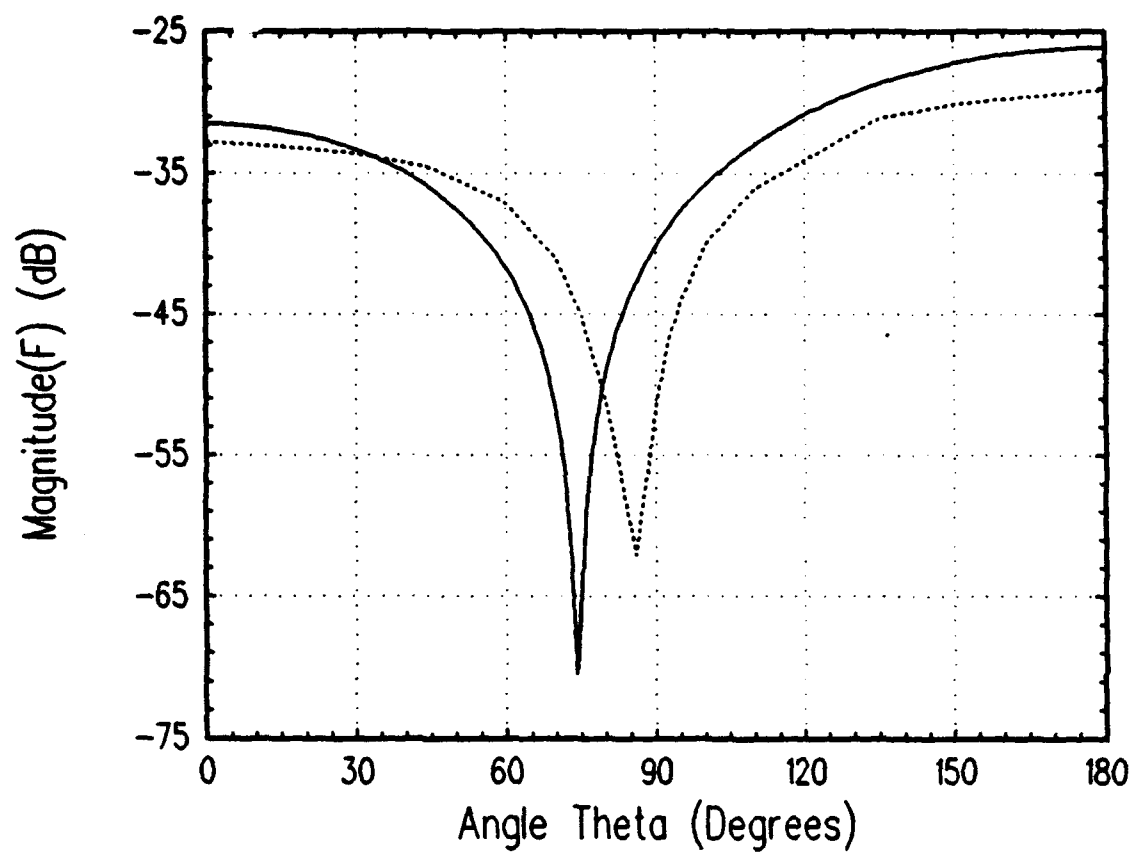Figure 8: The variation of the calculated (solid line) and reference (dotted line) magnitude of the normalized far-zone pattern in the xz-plane (E-plane) for the 81-element mesh.

39

concept that accurate local finite difference (FD) equations can be written at the boundary nodes if the geometry information can somehow be incorporated into the equations. Thus, a general FD equation is used at the boundary where the coefficients in the FD equations are unknown. These coefficients are then determined by the use of a sequence of "measures" called *metrons*. A more detailed discussion of this procedure is described in the next section.

a. Analysis of MEI for scattering from 2-D cylinders

To analyze the MEI, let us consider the problem of electromagnetic scattering from a two-dimensional perfectly conducting cylinder in free space (Figure 9). The boundary of the cylinder is defined to be ∂S_c. The formulation is derived only for the TM (E_z, H_x, H_y) polarization since the same procedure can be used for the TE case. The field solution is obtained from the solution of the Helmholtz equation for E_z. The grid surrounding the cylinder can either be a finite difference or a finite element grid. For this analysis, let us consider a finite difference grid. At the boundary of the grid, we cannot apply the traditional finite difference approximation because the traditional difference approximation requires grid points which are exterior to the grid. Thus, we must find another finite difference approximation which incorporates the radiation condition. The measured equation of invariance is based on the principle that a finite difference equation which couples the boundary nodes to the adjacent nodes can be formulated without using the traditional finite difference approximation. One possible coupling is the six-node coupling shown in Figure 9, where node 6 is coupled to nodes 1 through 5. To simplify the notation, the analysis is presented in terms of this coupling scheme without any loss of generality. The finite difference equation at node 6 can be written as

$$\sum_{i=1}^{6} a_i E_{zi}^s = 0 \tag{12}$$

where E_{zi}^s is the scattered electric field at node i and a_i are constant coefficients which must be determined. To find these coefficients, Mei et al. [6] use three postulates in which they conjecture that the finite difference equation in (12) is

1. Location dependent
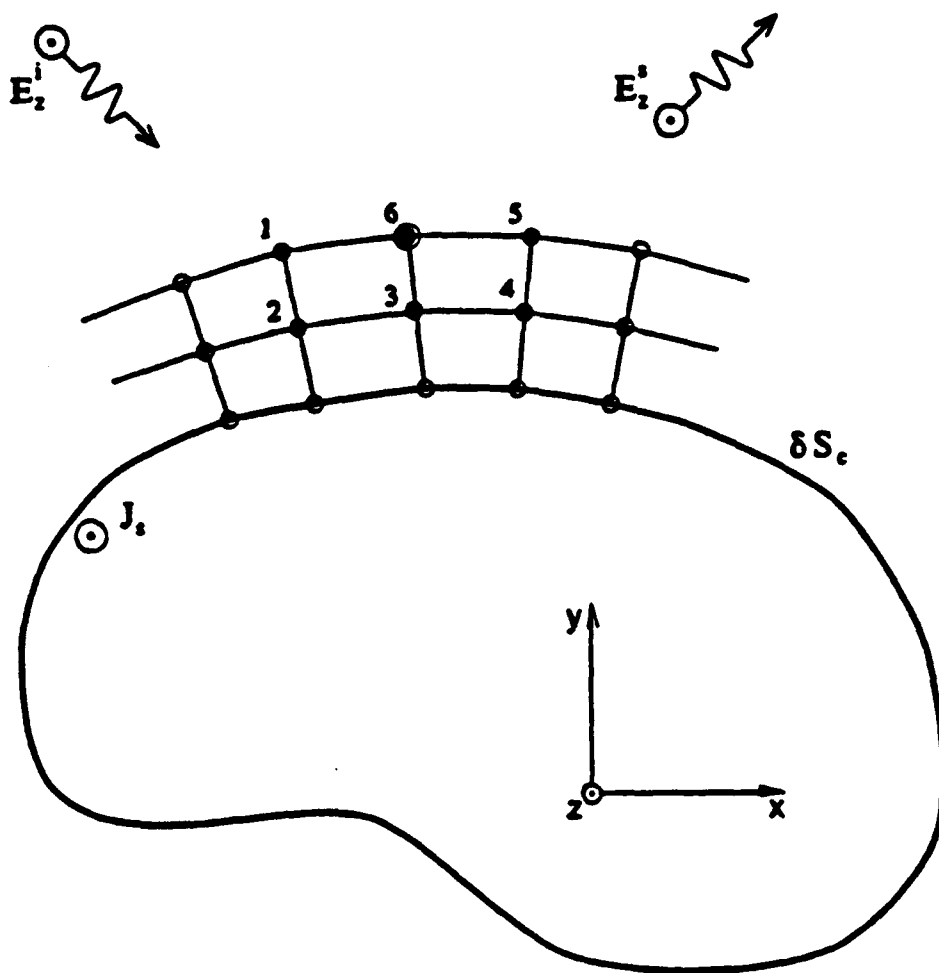
2. Geometry specific

40

Figure 9: Geometry for the measured equation of invariance.

3. Invariant to field excitation

The first two postulates can be shown to be true by numerical experimentation. These two postulates are also inherently incorporated into the global methods described in the previous section. The validity of the third postulate is not as clear. If the third postulate is true, then the coefficients in 12 can be determined from the field solutions at the six nodes due to five linearly independent excitations or metrons (only five are needed since the sixth coefficient is arbitrarily specified), which are denoted by the symbol Ψ_k. The five metrons represent five linearly independent surface current density distributions on the conducting cylinder. The metrons are usually chosen to be entire domain and to vary sinusoidally over the cylinder. For example, the choice in [6] is

$$\Psi_k = \begin{cases} \cos \pi k s & k = 0, 2, 4 \\ \sin \pi (k+1)s & k = 1, 3 \end{cases} \tag{13}$$

where $0 \leq s \leq 1$ describes the perimeter of the cylinder. Although the results presented in [6] seem to indicate that the third postulate is true, there were some unexplainable discrepancies in the numerical results. The reasons for these discrepancies can be determined from an analysis of the MEI.

An equation can be written relating E_{zi}^s to the induced electric surface current density J_z on the cylinder as follows,

$$E_{zi}^s = -j\omega\mu_0 \int_{\partial S_c} g(\vec{\rho}_i, \vec{\rho}\,')J_z(\vec{\rho}\,')d\ell' \tag{14}$$

where $\vec{\rho}_i$ is the position vector to node i and $g(\vec{\rho}_i, \vec{\rho}\,')$ is the free space Green's function which is given by

$$g(\vec{\rho}_i, \vec{\rho}\,') = \frac{1}{4j} H_0^{(2)}(k_0 |\vec{\rho}_i - \vec{\rho}\,'|) \tag{15}$$

The variable k_0 is the free space wave number given by $k_0 = \omega\sqrt{\mu_0\epsilon_0}$. The above equations are for the TM polarization. For the TE polarization, we must use $\hat{n} \cdot \nabla g$ where $\hat{n}$ is the unit normal from the conductor surface. Equation (14) is substituted into 12 to obtain

$$\sum_{i=1}^{6} a_i \int_{\partial S_c} g(\vec{\rho}_i, \vec{\rho}\,')J_z(\vec{\rho}\,')d\ell' = 0 \tag{16}$$

Recognizing the fact that $g(\vec{\rho}_i, \vec{\rho}\,') = g(\vec{\rho}\,', \vec{\rho}_i)$, we rewrite 16 as

$$\int_{\partial S_c} \left[\sum_{i=1}^{6} a_i g(\vec{\rho}\,', \vec{\rho}_i) \right] J_z(\vec{\rho}\,')d\ell' = 0 \tag{17}$$

The term inside the brackets has a special physical significance. It represents the electric field on ∂S_c due to six line sources of weights a_i located at the corresponding nodes i. Let us define E_{null} to be

$$E_{null}(\vec{\rho}\,') = \sum_{i=1}^{6} a_i g(\vec{\rho}\,', \vec{\rho}_i) \qquad \vec{\rho}\,' \in \partial S_c \tag{18}$$

In order for the third postulate to be true, a set of coefficients a_i must be found such that 17 is true for all possible excitations, i.e., all possible $J_z(\vec{\rho}\,')$ for $\vec{\rho}\,' \in \partial S_c$. This is only possible in the instance that

$$E_{null}(\vec{\rho}\,') = 0 \qquad \vec{\rho}\,' \in \partial S_c \tag{19}$$

However, it is impossible to choose a set of coefficients a_i such that 19 is satisfied. Thus, the third postulate is incorrect. It should be noted that we use the notation E_{null} in 18 since the desired value of E_{null} is zero.

Although the third postulate is wrong, the numerical results obtained from this method are still accurate. A detailed explanation for this accuracy in the form of a numerical study is provided in [7]. From this analysis, we see that the accuracy is dependent on the choice of metrons. It is expected that future research in the MEI will be in the development of more sophisticated metrons.

b. The use of the MEI for bodies of revolution

For the body of revolution problem, the geometry of the scatterer is invariant with respect to ϕ, however, the fields are functions of ϕ. It is useful to express the electric and magnetic fields in their Fourier modes in ϕ, because we will then have a series of modes which are invariant in ϕ. Let us consider the ϕ components,

$$E_\phi(\rho, \phi, z) = \sum_{m=-\infty}^{\infty} e^m(\rho, z) e^{jmphi} \tag{20}$$

$$H_\phi(\rho, \phi, z) = \sum_{m=-\infty}^{\infty} h^m(\rho, z) e^{jm\phi} \tag{21}$$

where the $\exp(j\omega t)$ time variation has been suppressed. Now instead of solving a three dimensional FEM problem we will be able to solve a series of two dimensional problems for e^m and h^m, since both these terms are independent of ϕ. In this work, the coupled azimuthal
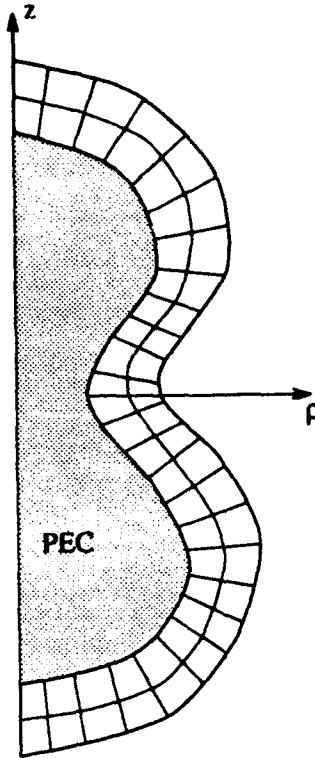
43

Figure 10: Sample body of revolution and mesh.

potential (CAP) formulation is used to perform the finite element analysis. This analysis is described in a previous paper [8]. The geometry for the problem is shown in Figure 10.

The MEI boundary conditions are based on the postulate, that for each node on the truncation boundary there exists a linear relation,

$$\sum_{i=0}^{N-1} (a_i e_i^{m,s} + b_i \eta h_i^{m,s}) = 0 \tag{22}$$

where $e_i^{m,s}$ and $h_i^{m,s}$ are the scattered electric and magnetic fields, respectively, for mode m, where $i = 0$ is the subscript of the node of interest and $i = 1$ to $i = N - 1$ are those of neighboring nodes. This means that a nodal value on the truncation boundary will be coupled only to values at the neighboring nodes. The free space impedance η is placed explicitly in 22 to properly scale b_i relative to a_i.

To define the MEI equation, we still need to find the coefficients a_i and b_i for each nodal value. To obtain geometry specific measuring functions a surface current density $\vec{J}^n(\vec{r}')$ on the scatterer surface, which is commonly referred to as a metron, is used. Note that in Equation (22) we are free to multiply by a constant and choose one of the coefficients. Thus,

44

$2N - 1$ unknowns must be determined. By choosing $2N - 1$ linearly independent metrons, we can form a $2N - 1$ by $2N - 1$ matrix equation to solve for the $2N - 1$ unknowns. It is also possible to use more than N metrons and then find a solution for the overdetermined system, but this is not done here.

To find the a_i's and b_i's we will now need measuring functions for both the electric and magnetic fields. Consider the electric vector potential $\vec{A}$ due to a metron $\vec{J}^n$ ($n = 1, \ldots, 2N - 1$),

$$\vec{A}^{m,n} = \int_{\partial S} \int_0^{2\pi} \frac{e^{-jk|\vec{r}-\vec{r}'|}}{4\pi|\vec{r}-\vec{r}'|} \vec{J}^n(\vec{r}')e^{jm\phi'} \, d\phi' \, d\ell' \tag{23}$$

where $\vec{r}$ is the observation point, and $\vec{r}'$ is the source point. We can now use the vector potential to solve for the measuring functions $e^{m,n}$ and $\eta h^{m,n}$, which are the field values at the nodes on, and just inside, the truncation boundary due to the metron $\vec{J}^n$, is

$$e^{m,n} = \hat{\phi} \cdot \left(\frac{\eta}{jk} \nabla \times \nabla \times \vec{A}^{m,n} \right) \tag{24}$$

$$\eta h^{m,n} = \eta \hat{\phi} \cdot \left(\nabla \times \vec{A}^{m,n} \right). \tag{25}$$

Substituting these measuring functions back into the MEI equation, we can solve for the coefficients a_i and b_i. The metrons used are given by

$$\vec{J}^n = \begin{cases} \hat{\phi} \sin\left[(n+1)\theta/2\right] & n \text{ odd} \\ (\hat{n} \times \hat{\phi}) \sin\left[n\theta/2\right] & n \text{ even} \end{cases} \tag{26}$$

where θ is a parametric mapping of ∂S to $[0°, 180°]$ (See Figure 10). In the case where the geometry is spherical, θ becomes one of coordinates in the spherical coordinate system. The metrons are chosen so that there is no net flow of current into the single point on the axis.

To demonstrate the accuracy of the MEI, two results are presented. In both cases, results are compared to those obtained from a method of moments body of revolution code [9]. The first is the plane wave scattering from a finite perfectly conducting circular cylinder with a radius of 5 wavelengths and a length of 5 wavelengths. The magnetic field H_ϕ on the surface of the cylinder is plotted in Figure 11. The results are close except near the top ($\theta = 0°$) and bottom ($\theta = 180°$) of the cylinder, where we expect the method of moments code to be incorrect due to its formulation. The second problem is a plane wave incident on a perfectly conducting cone (Figure 12). The results in this case do not agree as well as the previous

45

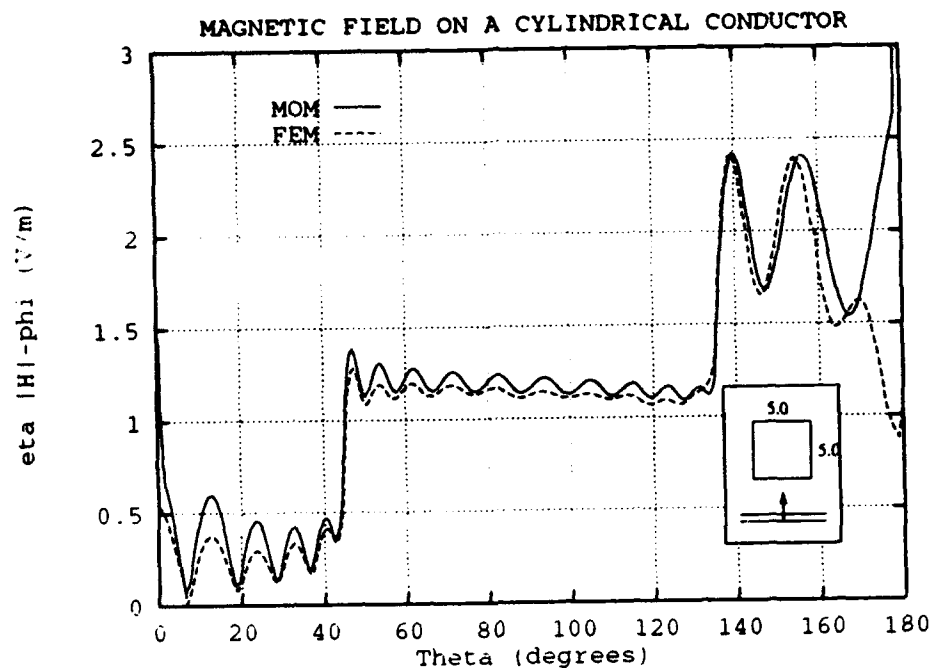**Figure 11: Magnetic field on the surface of a conducting cylinder, using sinusoidal metrons** ($\theta^{inc} = 180°$, $R = 2.5\lambda$, $H = 5.0\lambda$, Mesh: 20 nodes/λ, 5 layers of nodes).
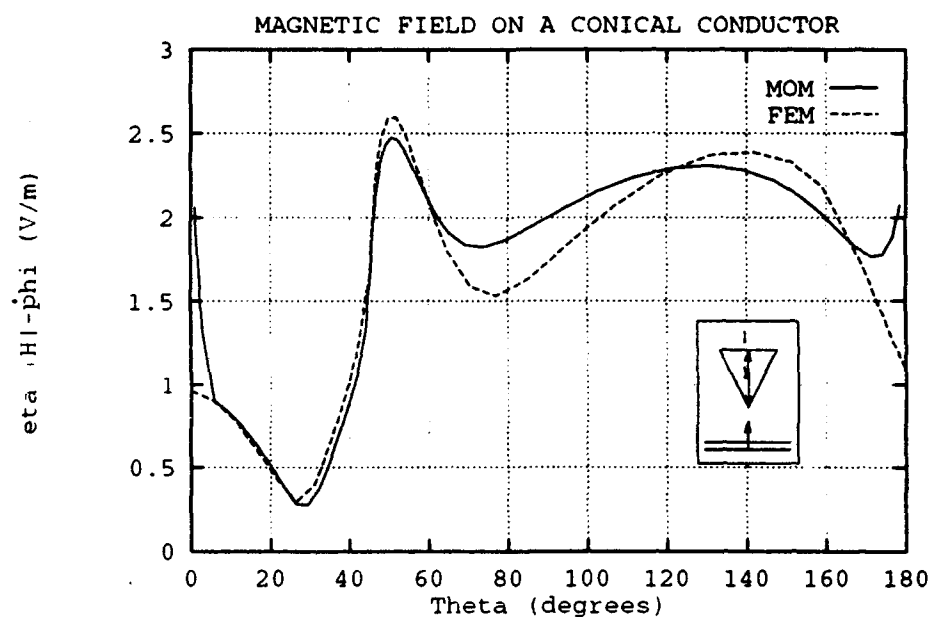

Figure 12: Magnetic field on the surface of a conducting cone, using sinusoidal metrons ($\theta^{inc} = 180°$, $R = 5.0\lambda$, $H = 1.0\lambda$, Mesh: 20 nodes/λ, 5 layers of nodes).
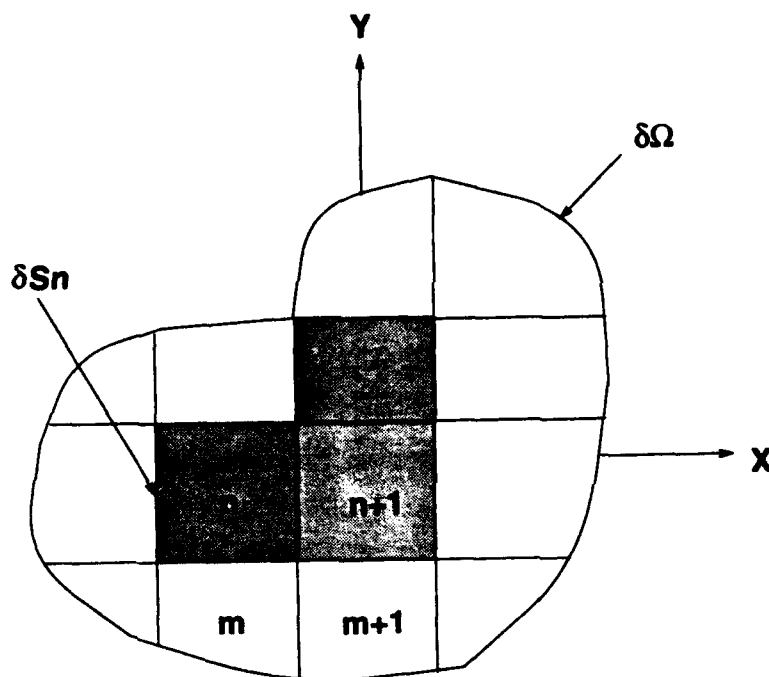
46

Figure 13: The partitioned solution domain.

results. It is evident that the MEI boundary condition is only approximate. A more detailed discussion of the MEI applied to the body of revolution is currently in preparation [10].

4. A Sequential and Parallel Implementation of the Partitioning Technique

In the 1992 JSEP annual report, the partitioning finite element technique was described for scattering from a two dimensional infinitely long cylinder. The partitioning was performed along only one of the dimensions, and results were presented to show the improvement in *efficiency compared to a direct finite element solution* based on a banded matrix solver. A journal paper has been accepted based on this work [11].

In this past year, the partitioning finite element techniques has been extended to allow partitioning to be performed along both dimensions (two-way partitioning). A sample partition is shown in Figure 13. It is expected that a two-way partition will be more efficient than a one-way partition based on a complexity analysis. We have also begun using sparse matrix solvers based on a nested dissection ordering of the matrix [12]. As we will see from the numerical results, The sparse solver is much more efficient than a banded solver. To

Table 1: Time comparison for solving the entire body vs. the partitioned body.

solution	entire method		partition technique		
domain	time(sec)		subregion	time(sec)	time(sec)
	banded	sparse		general	special
4λ sq	5.1	1.006	$.5\lambda$ sq	1.21	0.772
			1λ sq	1.705	1.358
8λ sq	106.893	5.774	$.5\lambda$ sq	5.645	2.762
			1λ sq	7.968	3.922
12λ sq		16.266	$.5\lambda$ sq	14.180	7.039
			1λ sq	19.364	7.917

test the performance of the partitioning technique, we consider square computation domains of various sizes. The computation region is assumed to contain a plane wave propagating through free space. This choice allows us to use either a Dirichlet or Neumann boundary condition on the computation boundary, thereby removing the computation of the boundary condition from consideration.

In Table 1, timing results on a Cray YMP/864 supercomputer are presented for three different cases. The *entire technique* refers to the traditional finite element method where no partitioning is used. The first thing to note is that the banded solver is very inefficient compared to the sparse solver. In the partitioning technique, the geometry is divided into either 0.5λ by 0.5λ sections or 1.0λ by 1.0λ sections where λ is the wavelength. The times for the partitioning technique are divided into the general case and the special case. In the general case, each section is assumed to be different from every other section. However, in the special case, every section is assumed to have the same shape and material properties. Thus, for geometries containing large regions of homogeneity, the computation time is closer to the special case. It is evident from Table 1 that the partitioning technique is much more efficient than the entire technique with a banded solver and potentially more efficient than the entire technique with a sparse solver. In fact, as the geometry size increase, the partitioning technique should become more efficient relative to the entire technique with the sparse solver.

Table 2: Memory comparison for solving the entire body vs. partitioned body.

entire body	Memory(Mword)		subregion	Memory(Mword)
	banded	sparse		
4λ sq	0.625	0.557	.5λ sq	0.0553
			1λ sq	0.0348
8λ sq	4.802	2.805	.5λ sq	0.385
			1λ sq	0.175
12λ sq	15.987	7.068	.5λ sq	1.118
			1λ sq	0.541

One of the greatest advantages of the partitioning technique is its small memory requirements. In Table 2, the memory requirements are presented. The tremendous decrease in memory requirements is due to the fact that the solution on each section can be handled sequentially.

The partitioning technique is ideally suited for parallel computers since most of the computation tasks for each section are independent of the other sections. The interaction between the separate section occurs only at the final step, where the sections are joined by means of a coupling matrix. Thus, each section can be placed on a single processor, and the independent computations are performed without any interprocessor communication. The interprocessor communication only occurs in the evaluation of the coupling matrix. The coupling matrix is solved with a sparse matrix algorithm specifically designed to balance the computation load and minimize the interprocessor communication. The performance of the partitioning technique on the Intel Delta machine operated by the Concurrent Supercomputer Consortium is demonstrated on an 8λ by 8λ computation domain, where the subdomains are 1λ by 1λ. The initial results are shown in Table 3. Although the computation domain is small relative to the number of processors considered, the results still show good speedup. It is expected that with a larger computation domain, the speedup will be considerably better. We are currently testing more cases on the parallel machine.

Table 3: Time performance on Delta machine. 8λ by 8λ computation domain divided in 1λ by 1λ sections.

No. of Processors	Time (sec.)
2	54.05
4	29.12
8	17.55
16	11.57
32	7.83

References

[1] A. C. Cangellaris and R. Lee, "The Bymoment Method for Two-Dimensional Electromagnetic Scattering," *IEEE Trans. Antennas Propagat.*, AP-38, pp. 1429-1437, September 1990.

[2] C. Hafner, "MMP - A Program Package Based on the Generalized Multipole Technique (GMT)," *Proc. IEEE APS Conference*, San Jose, 1989.

[3] P. Leuchtmann, "A Completely Automated Procedure for the Choice Of Functions in the MMP Method," *Proc. Int. Conference Comp. Meth. Flow Anal.*, Okoyama, September 1988.

[4] M. A. Morgan, C. H. Chen, S. C. Hill, and P. W. Barber, "Finite Element-Boundary Integral Formulation for Electromagnetic Scattering," *Wave Motion*, vol. 6, pp. 91–103, 1984.

[5] T. K. Sarkar, E. Arvas, and S. Ponapalli, "Electromagnetic Scattering from Dielectric Bodies," *IEEE Trans. Antennas Propagat.*, vol. AP-5, pp. 673–676, May 1989.

[6] K. K. Mei, R. Pous, Z. Chen, Y. W. Liu, "The Measured Equation of Invariance: A New Concept in Field Computation," Joint IEEE AP-S International Symposium and URSI Radio Science Meeting, Chicago, IL, July, 1992.

[7] J. Jevtic and R. Lee, "A Theoretical and Numerical Analysis of the Measured Equation of Invariance," accepted to *IEEE Trans. Antennas and Propagat.*

[8] M. A. Morgan, S. K. Chang, and K. K. Mei, "Coupled Azimuthal Potentials for Electromagnetic Field Problems in Inhomogeneous Axially Symmetric Media," *IEEE Trans. Antennas Propagat.*, pp. 202-214, May 1977.

[9] C. W. Chuang, "A Moment Method Computer Program for the Radiation and Scattering by a Conducting Body of Revolution," Technical report, The Electroscience Lab., The Ohio State University, Columbus, 1992.

[10] T. Barkdoll and R. Lee, "Finite Element Analysis of Bodies of Revolution using MEI Boundary Conditions," in preparation.

[11] R. Lee and V. Chupongstimun, "A Partitioning Technique for the Finite Element Solution of Electromagnetic Scattering from Electrically Large Dielectric Cylinders," accepted to *IEEE Trans. Antennas Propagat.*

[12] A. George and J. W. Liu, *Computer Solution of Large Sparse Positive Definite Systems*, Prentice-Hall, Englewood Cliffs, NJ, 1981.

5. Finite Element Studies — JSEP Publications

Accepted refereed journal papers:

1. R. Lee and T.T. Chia, "Analysis of Electromagnetic Scattering from a Cavity with a Complex Termination by Means of a Hybrid Ray-FDTD Method," *IEEE Transactions on Antennas and Propagation.*

2. U. Pekel and R. Lee, "An A Posteriori Error Reduction Scheme for the Three Dimensional Finite Element Solution of Maxwell's Equations," *IEEE Trans. Microwave Theory and Techniques.*

Oral presentations:

1. R. Lee and T.T. Chia, "A Hybrid Ray/FDTD Method for Computing Electromagnetic Scattering from an Engine Cavity with a Complex Termination," 9th Annual Review of Progress in Applied Computational Electromagnetics, Monterey, California, March 1993.

2. Y.S. Choi-Grogan and R. Lee, "A Sequential and Parallel Implementation of a Partitioning Finite Element Technique for Electromagnetic Scattering," International IEEE AP-S Symposium and URSI Radio Science Meeting, Ann Arbor, Michigan, June 28–July 2, 1993.

3. T.L. Barkdoll and R. Lee, "Finite Element Analysis of Bodies of Revolution using the Measured Equation of Invariance," International IEEE AP-S Symposium and URSI Radio Science Meeting, Ann Arbor, Michigan, June 28–July 2, 1993.

4. J. Jevtic and R. Lee, "Higher Order Divergenceless Edge Elements," International IEEE AP-S Symposium and URSI Radio Science Meeting, Ann Arbor, Michigan, June 28–July 2, 1993.

5. J. Jevtic and R. Lee, "An Analysis of the Measured Equation of Invariance," International IEEE AP-S Symposium and URSI Radio Science Meeting, Ann Arbor, Michigan, June 28–July 2, 1993.

VI. HYBRID STUDIES

Researchers:

P.H. Pathak, Professor	(Phone: 614/292-6097)
R. Rojas, Senior Research Associate	(Phone: 614/292-2530)
R. Lee, Assistant Professor	(Phone: 614/292-1433)
R.J. Burkholder, Post-Doctoral Researcher	(Phone: 614/294-9285)
M. Hsu, Graduate Research Associate	(Phone: 614/294-9284)
P. Munk, Graduate Research Associate	(Phone: 614/294-9279)
M. Otero, Graduate Research Associate	(Phone: 614/294-9277)

1. Introduction

The prediction of the EM radiation, scattering and propagation effects in increasingly complex environments whose overall dimensions are electrically large is a challenging task, because neither the high nor the low frequency techniques alone can, in general, provide useful solutions to describe such effects in a tractable and efficient manner. Thus, it becomes necessary to consider ways to break up the complex radiation, scattering and propagation configurations being analyzed into subdomains which can be classified as being high or low frequency regions depending on whether those individual regions are electrically large or small, respectively and then analyze these subdomains efficiently using separate methods or procedures which are best suited for it. Of course, these techniques must then be systematically combined in a self-consistent fashion to provide the desired solution for the entire configuration. Broadly speaking, such a systematic combination of different methods or techniques for analyzing any given complex radiating system may be referred to as a hybrid method of analysis. It could happen that an analysis of some of the subdomains of the entire complex radiation, scattering and propagation environment may itself require a hybrid treatment; in those cases, the systematic combination of such hybrid techniques to deal with the entire configuration may then be referred to as a super-hybrid method. For example, one may consider analyzing the phenomenon of EM radiation or scattering associated with a modern aircraft type of configuration, which is rather complex in that it consists of several antennas, radomes and other windows, jet inlet and exhaust cavities, etc., in addition to its

52

overall fuselage and control surfaces. It is possible to efficiently analyze the effects of the airframe, antennas, radomes, inlets, etc., separately using a hybrid combination of appropriate high and low frequency methods for each part, and then systematically combine these effects via a super-hybrid scheme to deal with the entire aircraft. Another example of the prediction of the interaction of EM waves with a complex structure is that which occurs in a shipboard environment containing a variety of large and small antennas. At present, work is in progress to develop useful hybrid schemes to predict: 1) the behavior of microstrip antennas as well as radome covered conformal slot arrays including feed networks, 2) the radiation and scattering of waves associated with complex aircraft and missile shapes, 3) the topside field distribution on ship models illuminated by large shipboard aperture antennas, and 4) the scattering by relatively arbitrarily shaped inlet cavities containing complex engine terminations. The present research work has built upon the initial ideas and concepts which led to the original hybrid combination of the asymptotic high frequency UTD technique (see the area of Diffraction Studies) with the moment method (MM) procedure for solving the low frequency integral equations for radiation/scattering as developed earlier at The Ohio State University [1, 2]. Solutions to a wide variety of additional useful topics still remain to be explored by hybrid methods; these will be addressed in the future phases of this study as the work in hybrid studies which is currently being pursued nears completion and lays the foundations for dealing with the next phase. The current accomplishments are reviewed next in slightly more detail.

2. Hybrid Analysis of Conformal Antenna Configurations

A hybrid MM-UTD method was developed previously under JSEP so that it could be implemented to efficiently analyze a large but finite array of stripline dipoles, patch antennas or other stripline antenna configurations on planar single and double layer grounded material substrates [3]–[5]. A direct numerical solution of such configurations using integral equation or differential (ie., finite difference or finite element) schemes would become rapidly intractable with an increase in the number of planar array elements especially at high frequencies. The hybrid procedure developed in [3]–[5] would on the other hand not suffer from any such limitations. During the present period, the previous work in [3]–[5] has been

extended to deal with slot arrays in a planar perfectly conducting screen and covered by a material superstrate that can be used for impedance matching and also as a radome.

The latter MM-UTD type hybrid solution is based on the development of an efficient closed form asymptotic (UTD type) aperture dyadic Green's function for a material coated ground plane containing an aperture; this Green's function is used as the kernel of the integral equation in the MM formulation of this slot array configuration. It is noted that the exact Green's function in this case is conventionally given in terms of a very slowly convergent Sommerfeld type integral which makes it almost intractable to treat large slot arrays with a material coating. The MM-UTD type hybrid technique can be employed to very efficiently analyze the performance of a large but finite array of slots in a planar conducting screen covered by a uniform material layer; also, it can accurately predict the scan performance of such arrays. It is seen from the literature that the performance of large (but finite) arrays is usually estimated via an infinite (periodic) array solution which is then modified to account for the finiteness of the array (i.e., the array edge effects) in an approximate fashion. This procedure is usually employed because the solution for the infinite periodic array is tractable as it restricts the unknowns in the MM solution to only a "unit cell" in the periodic array, and the effects of periodicity are rigorously accounted for using Floquet's theory. In contrast, the hybrid MM-UTD type solutions developed here for printed antennas and slots can deal very efficiently with a very large array of such radiating elements and automatically account for the array edge effects. It is proposed to compare the commonly used infinite array solution with the one based on the present hybrid approach for large finite arrays to see if there are significant differences between these two approaches especially for large scan angles where the edge effects can become important. As a further extension to this work, solutions have been obtained for the dyadic Green's functions that correspond to the fields of electric or magnetic point current sources near material coated perfectly conducting cylinders and spheres. Presently, the development of closed form asymptotic (UTD type) representations for these Green's dyadics for curved coated conducting surface are in progress. It is expected that once the challenging task of obtaining asymptotic estimates for the fields which remain valid even in the relatively close proximity of the point sources is completed, they will provide the same degree of versatility for treating a large finite array of antennas

54

(printed dipoles, patches, or slots) on material coated conducting cylindrical and spherical surfaces via a hybrid MM-UTD scheme as done for the corresponding planar cases discussed above. Furthermore, the UTD-like asymptotic form of the Green's functions for coated cylindrical and spherical surfaces can be extended via UTD concepts to treat antenna arrays located on convex conducting surfaces of variable curvature such as those encountered on the fuselages of aircraft and missile shapes. Such an extension of the canonical cylinder and sphere solution was performed previously under JSEP to deal successfully with the radiation from and mutual coupling between antennas on uncoated convex conducting surfaces of variable curvature [3]; the corresponding extension for coated convex surfaces is much more involved. Once the hybrid MM-UTD technique is completely developed for dealing with antennas and arrays of antennas on coated convex conducting boundaries of non-constant curvature, then it will provide a very powerful approach for the analysis and design of large finite conformal antenna arrays on such structures which otherwise cannot be handled even approximately using a periodic (or infinite) array analysis as has been done for the planar case in the literature since a variable surface curvature in general totally destroys periodicity. As a further extension, it is planned to include the effect of feed lines into the techniques for handling conformal arrays using the above mentioned hybrid MM-UTD type analysis. Such an integration will be made possible with the solutions that have been obtained recently for describing the waves on coplanar waveguides (CPW), slot lines, strip lines, etc.; these feed line solutions developed under this hybrid studies unit of JSEP have already been described in the previous annual report. The advantage of this hybrid approach will be that the unknowns in the MM will be limited to the antenna elements only (because of the UTD-like Green's function which will be incorporated as the kernel of the integral equation being solved by the MM procedure) and to just a few unknowns corresponding to the coupling amplitudes of the known behavior of the fields of modes on the array feed lines near and far from any feed line discontinuities, and to a minimal number of conventional MM subsectional basis set, if at all necessary, for describing the fields near the line discontinuities. Thus, a very efficient, physically appealing and accurate prediction of the phenomena of EM radiation, mutual coupling, and scanning in the very general case of large conformal arrays on convex

conducting surfaces of variable curvatures and with a uniform material coating will become available via the proposed hybrid procedure being developed here.

3. Hybrid Analysis of Radiation/Coupling Associated with Large Antennas in a Complex Environment

A generalized ray expansion (GRE) was developed previously under JSEP to deal with the EM scattering from open cavities [6]. That GRE is now being utilized along with some of its extensions and modifications which are currently in progress to predict the field behavior of large antennas (e.g., electrically large electronically and/or mechanically scanned phased arrays; mechanically scanned large reflector antennas, etc.) in a relatively complex environment. As described in the previous annual report, the large antennas are replaced by a set of equivalent sources over an appropriate mathematical surface which encapsulates the antenna so that the equivalent sources now radiate essentially the same field external to that surface as does the original antenna. The equivalent sources are found, for example, via a simple and highly efficient Gaussian expansion of the fields on the physical aperture of the antenna which are assumed to be known. The coefficients of the relatively few Gaussian elements required in this expansion are determined in a straightforward manner via Galerkin's method. The near fields of the antenna, which directly provide the equivalent sources over the encapsulating mathematical surface, are then found, by evaluating the radiation integrals containing the Gaussian expansion, in closed form. It is interesting that this closed form near field solution is valid at distances much closer to the physical antenna aperture than the conventional Fresnel zone distance. Furthermore, this near field solution is also automatically valid everywhere in the intermediate and far zone. The latter property provides one with a very efficient near field to far field transformation as a useful by-product. However, Gaussian beam (GB) techniques are not utilized in the present work to describe the fields radiated from the equivalent sources which are defined over the mathematical surface encapsulating the large antenna in question. Only the equivalent sources are represented in terms of closed form expressions for the fields radiated from the relatively few Gaussian aperture elements that are used in the aperture field expansion. It is noted that other types of Gaussian aperture elements (such as those based on a Gabor expansion) would not lead

to as efficient an expansion as the one developed here, because in the present approach the expansion is not required to synthesize any discontinuities that might be present at the edges of the physical aperture surface field distribution. In the present work, the GRE and its modifications (which are currently under study) are being considered for representing the fields radiated by the equivalent sources over the encapsulating mathematical surface so that ray methods can be employed to predict the effects of complex obstacles illuminated by the antenna. The advantage of the GRE concept is that one does not have to recompute the paths of rays launched from a discrete array of points on the encapsulating surface even if the antenna is scanned mechanically or electronically. The ray paths are independent of the antenna orientation or excitation; they depend only on the given geometry of the complex environment in the presence of the antenna. The initial ray launching amplitude of course depends on the antenna orientation and excitation. The development of a hybrid analysis of some complex structures which can be illuminated by such antennas has recently begun. Some examples of such structures are masts or other objects which can be modelled by the UTD. The conducting mast could be solid and impenetrable or be made up of a zig-zag or triangular array of finite length rods. A hybrid MM-UTD like analysis is currently being developed for such masts. The latter is of interest for predicting the effects of large antennas in shipboard environments. An application of this novel hybrid Gaussian-GRE-UTD approach being developed here is indeed useful for dealing with shipboard antennas; the latter application and associated code development that fit some specific needs are being currently funded under a separate grant from the Navy. Details of the hybrid Gaussian-GRE-UTD approach discussed above will be reported by the end of the next period.

4. Hybrid Analysis of Radiation and Scattering Associated with Airborne/Spaceborne Objects

The development of a hybrid method based on the combination of MM-UTD has been nearly completed for dealing with the radiation by antennas on or the scattering from a configuration consisting of a perfectly conducting circular or elliptical cylinder to which can be attached perfectly conducting plates of relatively arbitrary shapes. Such a configuration can simulate a generic aircraft fuselage with wings and horizontal as well as vertical stabilizers, or a

missile shape with fins. This hybrid procedure is efficient because it employs an asymptotic (or UTD) closed form representation for the fuselage Green's function; thus, the unknowns in the MM solution of the governing integral equation which contains this Green's function as the kernel are restricted to only the control surfaces (wings and stabilizer). In contrast, a conventional MM solution would utilize a free space Green's function as the kernel of the governing integral equation thereby requiring one to solve for the unknown currents induced over the entire aircraft/missile structure in question, thus making it practically intractable for use at high frequencies. For example, a typical aircraft is several hundred wavelengths long at X-band; this leads to a prohibitively large number of unknowns (about 16 per square wavelengths if subsectional basis functions are used) over the entire surface of such an aircraft. In contrast, the present hybrid MM-UTD drastically reduces the number of unknowns to only the control surfaces. In this hybrid scheme, it was necessary to extend the previously developed UTD for convex surfaces [2]–[4] that was valid only for source/observer either directly on or not close to the convex surfaces. The above extension was required because this hybrid MM-UTD must have a knowledge of both the extreme near, intermediate and far zone fields of sources which can be close to but not necessarily located directly on the convex boundaries. This UTD extension was reported in the previous annual report. During the present period, considerable effort has been expended to determine the regions of validity of the different extensions of the UTD corresponding to different source and observer regions since it was not possible to obtain a single expression valid uniformly for all source/observer locations with respect to the convex body, which would at the same time remain very efficient for computations. Due to the fact that the exact form of the error of the different extended UTD expressions which were developed is not known, a more heuristic approach based on numerical experiments was instituted to determine the various conical and cylindrical mathematical boundaries which define the regions of validity of each of these different extended UTD expressions. Such delineation of the various regions of validity for the extended UTD expressions are necessary for use in a hybrid MM-UTD based algorithm to obtain accurate numerical results. Indeed some numerical results pertaining to the scattering by a small fin on a circularly cylindrical conducting surface which have been obtained using the above hybrid MM-UTD are seen to compare very well with measurements. It is proposed

58

to extend this work next to include a UTD Green's function which is valid for a general convex surface to model a fuselage more accurately than is possible with just a cylindrical surface; this could also include the effects of the fuselage end cap (to simulate a transparent radome on the nose of the fuselage). Such a UTD Green's function will be developed under the unit on Diffraction Studies which deals with the paraxial radiation and diffraction associated with antennas near an elongated smooth convex surface with perhaps an end cap. Additional future extensions will include the integration of conformal antenna and antenna arrays, as well as the integration of inlet/exhaust cavities into the aircraft/missile structure via a super-hybrid scheme as discussed in the introduction. Furthermore, it is planned to achieve a further reduction in the number of MM unknowns (= the number of basis functions) on the control surfaces by incorporating a mix of a relatively few conventional subsectional MM basis set and an entire domain physical basis set (dictated by an anticipated UTD surface field behavior), rather than the larger number of conventional subsectional MM basis set currently in use within the hybrid MM-UTD for the generic aircraft/missile shape.

5. Hybrid Analysis of the Scattering of an Impedance Wedge in the Presence of a Material Body

The purpose of this analysis is to study the electromagnetic scattering characteristics of a material body in the presence of a wedge shaped object. This is a two dimensional problem where the wedge is of infinite extent and its faces can have different impedance boundary conditions. The material body is of arbitrary shape and can be inhomogeneous. The motivation for this effort is that the purely analytical results described in the Diffraction Studies section (diffraction by thin material edges/junctions and coated conducting edges) are limited to simple canonical shapes. Hybrid schemes such as the one described here will allow us to solve much more complicated configurations that are more realistic for practical applications. The results to be developed in this effort can be used in an existing optimization algorithm to synthesize a d____d frequency response of a wedge shaped material scatterer.

The main idea of the hybrid scheme presented here is to use the analytical results obtained under the Diffraction Studies section to obtain numerically efficient Green's functions which can them be used to develop integral equations with as few unknowns as possible. The

method of analysis that is being used is a method of moments/Green's function technique where the Green's function is that for a wedge with different impedance faces. The method of moments technique is used to solve for the field that is scattered by the material body. The major tasks to be accomplished in this project are to 1) solve for the two dimensional Green's function for the impedance wedge, 2) formulate an integral equation for the unknown scalar field inside the material body, and 3) implement a method of moments technique to solve the integral equation.

The following is an overview of what has been accomplished in the past year. Most of the work has been in developing the Green's function. There are no restrictions on the Green's function since it must be valid everywhere in space. Due to the fact that it will be called numerous times by the moment method technique, it is necessary for the Green's function to be in a form that is computationally efficient to evaluate, and this is where much of the effort has been spent [7].

The two dimensional Green's function for the impedance wedge is in the form of a double integral with an integrand that has many singularities. Because the integrand is, in general, a very complex expression, the integral cannot be evaluated in closed form. Each of the integrals depends on the location of either the source or the observation point. The contour of integration which pertains to the location of the observation point is along a Sommerfeld contour, while the contour of integration that pertains to the location of the source point is along a steepest descent path. The location of the source or observation points can be considered to be in one of three regions, either the near zone, intermediate, or far zone, which is determined with respect to their increasing radial distance from the wedge vertex. When the observation point is in the near zone, it is more efficient to numerically evaluate its associated integral along a deformed Sommerfeld contour. In fact, this integral can even be evaluated in closed form for the limiting case when the observation point approaches the wedge vertex. However, at larger distances from the wedge vertex, it becomes more efficient to numerically evaluate the integral along a steepest descent path. Therefore, for the case when the observation point is in the intermediate or far zones, the Sommerfeld contour is deformed to a steepest descent path through its saddle point. This integral is evaluated numerically using a very efficient Gaussian integration routine when in the intermediate

zone, and it is evaluated asymptotically when in the far zone. Similarly, the contour of integration pertaining to the source point is along a steepest descent path which is also deformed to its respective saddle point and is evaluated asymptotically when the source point is in the far zone and evaluated numerically otherwise. Further work is being done to obtain a representation for the Green's function which is more efficient to evaluate when both source and observation points are in the near zone.

Deforming the contours of integration in the double integral gives rise to many terms that contain single integrals. These integrals are evaluated in the same manner as mentioned above. Also, all of the singularities in the integrands are explicitly separated from the integrals and evaluated in closed form. The result is that we have various forms for the Green's function, each designed for maximum efficiency in computation depending upon the region for which it needs to be evaluated. Since the Green's function satisfies reciprocity, the above conditions also apply when the source and observation points are interchanged. A computer code has been written to evaluate the Green's function using the analytic expressions described above as well as a reference solution which uses a method of moments technique. The agreement between the two methods is very good.

A computer code has also been written which determines the scattered field, due to an incident plane wave, from an inhomogeneous material body in the presence of the wedge. This solution uses the specialized Green's function for the wedge described above. The current configuration for the material body is in the form of a dielectric slab of rectangular cross section where the relative dielectric constant can vary within the slab. The location of the slab with respect to the wedge is arbitrary. This will later be modified so that the material body can be of arbitrary shape and not limited to dielectric materials. In fact, the present integral equations will be modified so that chiral as well as anisotropic materials can be studied. The code has been verified for the limiting case when the impedance wedge becomes a perfectly conducting semi-infinite half plane. For this case, a comparison was made with a code developed by Dr. E.H. Newman for the case of plane wave scattering from an inhomogeneous rectangular dielectric slab in the presence of a PEC semi-infinite half plane. The agreement between the two codes is excellent.

61

6. Hybrid Analysis of Planar Guided Wave Structures

Most of the details of the research effort in this topic was reported last year. The results of this research efforts resulted in a PhD Dissertation [8] and two journal papers [9, 10]. The method used to perform the analysis of the propagation characteristics of planar transmission lines is referred to as the Wiener-Hopf/Generalized Scattering Matrix Technique (WH/GSMT). This method is applicable to transmission lines with large lateral dimensions. It can complement numerical schemes which are more efficient for small structures. The first paper [9] concentrates on introducing the method and only a few numerical results are shown. The goal of the second paper [10] is to demonstrate the versatility of the present full wave analysis scheme by applying it to a variety of planar transmission line configurations. *Note that the complex propagation constants for the transmission lines were obtained for the dominant as well as higher order modes.* This is in contrast to many published papers found in the literature where only the real part of the propagation constant is given for the dominant mode. Due to the analytical nature of the WH/GSMT, the results based in this method can be used as reference solutions for the more common numerical techniques. It it noted that as more advances are made in the analysis of electromagnetic diffraction by material bodies with edges, junctions, etc., those results can be used to analyze more complicated planar transmission lines by means of the present WH/GSMT.

7. Hybrid Ray/FDTD Method for Inlet Cavities

The use of ray methods coupled with the finite difference time domain (FDTD) method for scattering from jet inlet cavities was discussed in last year's report. In that report, we presented a preliminary description of the ray/FDTD method. The use of a hybrid method is ideal for a jet inlet cavity since the the cavity contains a portion which is simply shaped (the inlet duct) and a portion which is geometrically complex (the engine termination). The generalized ray expansion (GRE) method is used to model the duct while the FDTD method is used to model the termination. The major difficulty comes in the coupling between the two methods. Based on the work done this past year, we have developed several techniques for coupling the two methods. A detailed description of the coupling between the GRE method
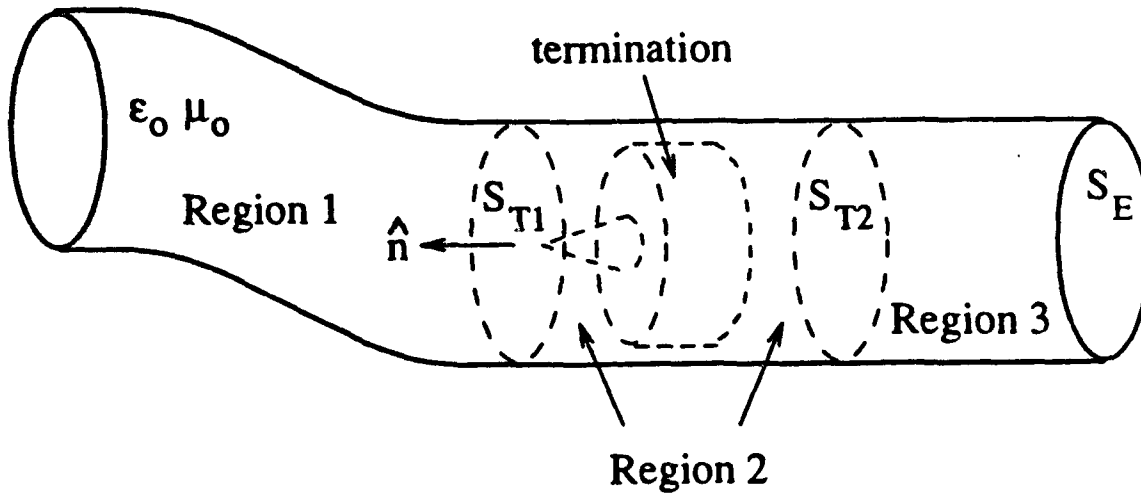
Figure 14: Geometry of cavity with termination.

and the FDTD method is provided below. The work on the hybrid ray/FDTD method has been accepted for publication [11].

As with most electromagnetic hybrid methods, the coupling between the individual methods has to be handled with care. Consider the cavity shown in Figure 14. The cavity has been divided into three regions corresponding roughly to the air intake, the engine, and the exhaust sections of a jet engine inlet. The imaginary surface S_{T1} separates Regions 1 and 2 while S_{T2} separates Regions 2 and 3. In Region 1, the cavity is assumed to be smoothly varying for high frequency methods, i.e., ray methods, to be valid. Ray tubes are traced from the aperture of the cavity to S_{T1} where they are summed to form a high frequency solution of the cavity fields across S_{T1}. This solution on S_{T1} is used as the excitation for the FDTD computation in Region 2.

We will now describe two approaches to the coupling between the GRE and the FDTD methods. Depending on the size of a ray tube when it reaches S_{T1}, it will either not intersect any of the FDTD grid points on S_{T1} or it will intersect one or more of those grid points. Therefore, different ray tubes will contribute differently to the total field of a grid point. Moreover, it is possible that some grid points will not have any ray tubes intersecting them.

As a result, the *incident* fields on S_{T1} evaluated via rays will not be smoothly varying. In order to obtain a smoothly varying as well as an accurate field on S_{T1}, the size of the ray tube can be restricted so that it will only intersect one FDTD grid point. Alternatively, some form of interpolation can be applied to the ray tubes that intersect more than one grid point. In both of these approaches, a ray tube is launched and tracked via its central ray to S_{T1}. The projected ray tube *area* (for the 3D case, *width* for the 2D case) on S_{T1} is then determined. If this area is greater than some specified area, A_p, the ray tube is subdivided and the process of tracking and determining the projected area of the smaller ray tubes is repeated. In the first approach, A_p is equal to the FDTD grid spacing (usually $\lambda/20$) for the 2D case so that if the projected ray tube *width* is less than A_p, that ray tube can intersect at most one FDTD grid point on S_{T1}. In such an event, the field specified by the central ray will be added to the intersected grid point. Ray tubes that do not intersect any grid point are ignored.

For the second approach, we use a larger value of A_p ($A_p = \lambda/4$). Since a larger ray tube may intersect more than one FDTD grid point on S_{T1}, its contribution to the field on S_{T1} is determined by converting its ray field into modal fields. Specifically, the contribution of the ray field to the modal coefficients are determined by integrating the ray field over the projected area of the ray tube assuming a linear phase variation in the field over the projected area with respect to the field of the central ray. This approach assumes that the fields on S_{T1} are expressible in terms of parallel-plate waveguide modes for 2D problems. This assumption can usually be satisfied by a suitable choice of S_{T1}. In realistic 3D problems, there is usually a narrow section in front of the termination which is cylindrical so that the fields in this narrow section can also be expressed in terms of modes. In any case, when the modal coefficients have been obtained by summing the contributions due to *all* the ray tubes, the desired field at each FDTD grid point on S_{T1} can be determined.

Comparing the two approaches, it is clear that the first approach requires more ray tracing (which means more computational time and storage) than the second approach because of the smaller A_p. However, once the rays are traced, the first approach uses only a simple summation of the ray fields to obtain the desired fields at the FDTD grid points on S_{T1}. The second approach is less efficient in this latter aspect as it has to compute the modal

coefficients and then sum the modal fields to get the desired fields. However, in realistic 3D problems, the first approach may not be viable because the amount of ray tracing can become excessive.

Another consideration in the coupling of the GRE and FDTD methods is the selection of a suitable time variation for the excitation since the former is a frequency-domain method while the latter is a time-domain method. There are two possible schemes for the time variation: the sinusoidal steady-state time variation and the pulsed (usually Gaussian or raised-cosine) time variation. For the steady-state FDTD, the ray solution on S_{T1} is evaluated only at a single frequency of interest. Based on the complex ray field solution at S_{T1}, the excitation can be made to vary sinusoidally with time. For the pulsed FDTD, there are two possible alternatives. For the first alternative, the ray solution on S_{T1} is computed over a range of frequencies corresponding to the frequency content of the pulse. The excitation can then be obtained by an inverse Fourier transform of the product of the ray solution and the Fourier transform of the pulse. This alternative is not attractive as the resultant inverse transform will have a wide time window with a number of significant pulses due to the different arrival times at S_{T1} of the reflected, diffracted and reflected-diffraction fields. A better alternative is to use a basis set (eg. modes) as excitation for the pulsed FDTD to characterize the termination section in terms of a termination scattering matrix. This scattering matrix, together with the ray solution on S_{T1} (expressed also in terms of the basis set), can then be used to find the cavity scattered field. The pulsed time variation scheme is more efficient for problems which require multiple frequency solutions while the steady-state scheme is more efficient for problems which require only a single frequency solution.

Regardless of the time variation used, the excitation produces a wave which propagates toward the termination and interacts with it. For the geometry shown in Figure 14, part of the wave may be transmitted to Region 3 through S_{T2} while the remainder is reflected back towards S_{T1}. If we assume that the waves leaving Region 2 through the imaginary surfaces S_{T1} and S_{T2} do not return, then an absorbing boundary condition can be applied in the FDTD computations at each of the two surfaces. The above assumption is reasonable as most jet engine inlets are shaped in such a way that there is very little energy that returns to Region 2 upon its exit from there. Otherwise, we can convert the waves leaving Region 2

back into rays (using GRE) and track those rays that return to Region 2. These returning rays act as an additional excitation.

The results based on this coupling scheme have been excellent for the two dimensional case. We have implemented the method for three-dimensional geometries and are currently validating the code with reference solutions.

References

[1] G.A. Thiele and T.H. Newhouse, "A Hybrid Technique for Combining Moments with the Geometrical Theory of Diffraction," *IEEE Trans. Antennas and Propagation*, Vol. 33, pp. 62-69, January 1975.

[2] W.D. Burnside, C.L. Yu and R.J. Marhefka, "A Technique to Combine the Geometrical Theory of Diffraction and the Moment Method," *IEEE Trans. Antennas and Propagation*, Vol. 33, pp. 551-558, July 1975.

[3] M.A. Marin and P.H. Pathak, "An Asymptotic Closed-Form Representation for the Grounded Double-Layer Surface Green's Function," *IEEE Trans. on Antennas and Propagation*, Vol. AP-40, pp. 1357-1366, November 1992.

[4] S. Barkeshli, P.H. Pathak and M. Marin, "An Asymptotic Closed-Form Microstrip Surface Green's Function for the Efficient Moment Method Analysis of Mutual Coupling in Microstrip Antenna Arrays," *IEEE Trans. on Antennas and Propagation*, Vol. AP-38, pp. 1374-1383, September 1990.

[5] M. Marin, S. Barkeshli and P.H. Pathak, "Efficient Analysis of Planar Microstrip Geometries using an Asymptotic Closed-Form of the Grounded Dielectric Slab Green's Function," *IEEE Trans. on Microwave Theory Techniques*, Vol. MTT-37, pp. 669-678, April 1989.

[6] P.H. Pathak and R.J. Burkholder, "High Frequency Electromagnetic Scattering by Open-Ended Waveguide Cavities," *Radio Science*, Vol. 26, p. 211-218, 1991.

[7] M.F. Otero and R.G. Rojas, "Scattering and Radiation in the Presence of a Material Loaded Impedance Wedge," 1993 IEEE APS/URSI International Symposium, Ann Arbor, Michigan, June-July 1993

[8] L.M. Chou, "A Novel Hybrid Full-Wave Analysis Method for Planar Transmission Lines Embedded in Multilayered Dielectrics–The WH/GSMT," PhD Dissertation, Department of Electrical Engineering, Ohio State University, Columbus, Ohio, December 1992.

[9] L.M. Chou, R.G. Rojas and P.H. Pathak, "WH/GSMT Based Full-Wave Analysis of Planar Transmission Lines Embedded in Multilayered Dielectric Substrates," accepted for publication, *IEEE Trans. on Microwave Theory and Techniques*.

[10] L.M. Chou and R.G. Rojas, "Dispersion and Lateral Leakage of Conductor Backed Coplanar Waveguides with Layered Substrate and Finite-Extent Lateral Ground Planes," submitted to *IEEE Trans. on Microwave Theory and Techniques*.

[11] R. Lee and T. T. Chia, "Analysis of electromagnetic scattering from a cavity with a complex termination by means of a hybrid ray-FDTD method," to appear in November, 1993 issue of *IEEE Trans. Antennas Propagat.*

8. Hybrid Studies — JSEP Publications

Published refereed journal papers:

1. M. A. Marin and P.H. Pathak, "An Asymptotic Closed-Form Representation for the Grounded Double-Layer Surface Green's Function," *IEEE Transactions on Antennas and Propagation*, Vol. 40, No. 11, pp. 1357–1366, November 1992.

2. P.H. Pathak and R.J. Burkholder, "A Reciprocity Formulation for the EM Scattering by an Obstacle Within a Large Open Cavity," *IEEE Transactions on Microwave Theory and Techniques*, Vol. 41, No. 4, pp. 702–707, April 1993.

Accepted refereed journal papers:

1. L.M. Chou, R.G. Rojas and P.H. Pathak, "WH/GSMT Based Full-Wave Analysis of Planar Transmission Lines Embedded in Multilayered Dielectric Substrates," *IEEE Trans. on Microwave Theory and Techniques*.

Oral presentations:

1. M.F. Otero and R.G. Rojas, "Scattering and Radiation in the Presence of a Material Loaded Impedance Wedge," International IEEE AP-S Symposium and URSI Radio Science Meeting, Ann Arbor, Michigan, June 28–July 2, 1993.

2. R.J. Burkholder and P.H. Pathak, "A Generalized Ray Expansion for Computing the EM Fields Radiated by an Antenna in a Complex Environment," International IEEE AP-S and National URSI meeting in Ann Arbor, Michigan, June 28–July 2, 1993.

3. P.H. Pathak, "EM Analysis of HF Scattering by and Coupling into Open Cavities," invited lecture, 11th Annual IEEE Benjamin Franklin Symposium in Philadelphia, Pennsylvania, May 1, 1993.

4. P.H. Pathak, "Asymptotic HF Techniques for EM Antenna and Scattering Analysis," invited lecture, Symposium on Mathematical Methods in Wave Scattering Theory, Faculty of Science and Engineering, Chuo University, Tokyo, JAPAN, September 3, 1993.